SCIENCE CHINA
Life Sciences

SPECIAL TOPIC
• REVIEW •

October 2012 Vol.55 No.10: 843–861
doi: 10.1007/s11427-012-4380-1

Engineering imaging probes and molecular machines for nanomedicine

TONG Sheng[1], CRADICK Thomas J.[1], MA Yan[2], DAI ZhiFei[2] & BAO Gang[1,2*]

[1]*Department of Biomedical Engineering, Georgia Institute of Technology and Emory University, Atlanta, GA 30332, USA;*
[2]*Department of Biomedical Engineering, College of Engineering, Peking University, Beijing 100871, China*

Received August 21, 2012; accepted September 10, 2012

Nanomedicine is an emerging field that integrates nanotechnology, biomolecular engineering, life sciences and medicine; it is expected to produce major breakthroughs in medical diagnostics and therapeutics. Due to the size-compatibility of nano-scale structures and devices with proteins and nucleic acids, the design, synthesis and application of nanoprobes, nanocarriers and nanomachines provide unprecedented opportunities for achieving a better control of biological processes, and drastic improvements in disease detection, therapy, and prevention. Recent advances in nanomedicine include the development of functional nanoparticle based molecular imaging probes, nano-structured materials as drug/gene carriers for *in vivo* delivery, and engineered molecular machines for treating single-gene disorders. This review focuses on the development of molecular imaging probes and engineered nucleases for nanomedicine, including quantum dot bioconjugates, quantum dot-fluorescent protein FRET probes, molecular beacons, magnetic and gold nanoparticle based imaging contrast agents, and the design and validation of zinc finger nucleases (ZFNs) and TAL effector nucleases (TALENs) for gene targeting. The challenges in translating nanomedicine approaches to clinical applications are discussed.

nanomedicine, imaging probe, contrast agent, drug delivery, designer nuclease

Citation: Tong S, Cradick T J, Ma Y, *et al*. Engineering imaging probes and molecular machines for nanomedicine. Sci China Life Sci, 2012, 55: 843−861, doi: 10.1007/s11427-012-4380-1

Nanomedicine is an emerging field that integrates nanotechnology, biomolecular engineering, biology, and medicine [1]. It focuses on the development of engineered nano-scale (1−100 nm) materials, structures and devices for better diagnostics and highly specific medical intervention in curing disease or repairing damaged tissues. As a basis for nanomedicine, nanotechnology is the science, engineering, and technology related to the understanding and control of matter at the nano-scale, and the development of materials, devices, and systems that have novel properties and functions due to their nano-scale dimensions or components. Nanotechnology also provides new abilities to measure, control and manipulate matter (including soft matter) at the nano-scale what was unthinkable with conventional tools. Owing to the size-compatibility of nano-scale structures with proteins and nucleic acids in living cells, nanomedicine approaches have the potential to provide unprecedented opportunities for achieving a better control of biological processes, and drastic improvements in disease detection, therapy, and prevention, thus revolutionizing medicine.

Over the last ten years or so, significant efforts have been made in the US, China, Europe and elsewhere to develop nanomedicine. For example, the US National Institutes of Health has developed a nanomedicine centers network, and invested a significant amount of research funding to nanomedicine development. Just in FY 2009 (Oct. 1, 2008−Sept. 30, 2009), the total NIH funding in nanotechnology/nanoscience projects was more than 410 million US dollars.

*Corresponding author (email: gang.bao@bme.gatech.edu)

Many potential applications of nanomedicine have been, or are being, explored, including nanoparticle-based molecular imaging probes for biological studies and disease detection; nano-carriers for targeted *in vivo* drug/gene delivery in more efficient therapy, and nuclease-based nano-devices for treating single-gene disorders. For basic biological studies, the development of new nano-scale tools and devices have the potential to permit imaging of cellular structures at the nano scale, rapid measurement of the dynamic behavior of protein complexes and molecular assemblies in living cells and animals, and a better control of intracellular machinery. It is expected that the multifunctional, targeted nanoparticles are capable of overcoming biological barriers to deliver therapeutic agents preferentially to diseased cells and tissues at high local concentrations, resulting in much enhanced efficacy and reduced toxicity. Nanomedicine approaches have the potential to allow clinicians to detect a disease in its earliest, most easily treatable, presymptomatic stage, and provide real-time assessments of therapeutic and surgical outcome. Nano-scale tools may also be used to quickly identify new disease targets for drug development and predict drug resistance.

In this review, we will focus on nano-structured and nanoparticle-based molecular imaging probes, including fluorescence imaging probes and nanoparticle contrast agents for MRI, PET, and CT, and molecular machines using engineered nucleases for gene targeting. Due to space limitations, this is not intended to be a comprehensive review, but rather a review of selected research topics in nanomedicine to highlight the diversity and innovation in the field. Other reviews of nanomedicine can be found in recent literature [2,3]. Although nanomedicine has the potential to revolutionize medicine, it is still in its infancy and significant challenges exist. Therefore, some of the major challenges that must be overcome are also discussed.

1 Fluorescence imaging probes

Fluorescence imaging probes have been widely used in biology and medicine. It is therefore not surprising that the development of nano-structured and nanoparticle-based fluorescence probes is one of the most active areas in nanomedicine. Described below are some of the fluorescence probes developed in recent years, including semi-conductor quantum dot (QD) based probes, and molecular beacons.

1.1 Quantum dot bioconjugates as fluorescence imaging probes

Semi-conductor quantum dots (QDs) are core-shell nanocrystals that have exceptionally bright fluorescence emission, with emission peaks tunable by the size of QD (typically 2–6 nm) (Figure 1); they have garnered much attention recently as an emerging tool for biomedical applications [4–23]. Since QDs were first rendered water-soluble [7,15], thereby making them relevant for biological studies in 1998, they have been applied to cell tracking studies [24,25], cancer imaging [13,26], flow-cytometry [27], and used to label membrane proteins [28,29]. The potential applications for QDs also extend to fluorescence-based detection of enzymatic activities, particularly when QDs are utilized as either a donor or an acceptor for fluorescence (or Förster) resonance energy transfer (FRET) [30–34]. QDs have large molar extinction coefficients (0.5×10^6–5×10^6 M^{-1} cm^{-1}) which makes them brighter probes under photon-limited *in vivo* conditions (where light intensities are attenuated by scattering and absorption). Since such extinction coefficients are 10–50 times larger than those of organic dyes (at 5×10^4–10×10^4 M^{-1} cm^{-1}), QD absorption rates are typically 10–50 times faster at the same excitation photon flux (number of incident photons per unit area). Due to this, individual QDs are 10–20 times brighter than typical organic dyes [7,10,15]. Therefore, it is possible to fluorescently image single individual QDs. An important aspect of QD labels is their extremely high photostability. QDs are several thousand times more stable against photobleaching than organic dyes, which allows real-time monitoring or tracking of intracellular processes over long periods of time (hours to days). Further, QDs have Stokes shifts (separation between excitation and emission peaks) as large at 300–400 nm [13]. This reduces interference from tissue autofluorescence in biological specimens, which often buries organic

Figure 1 A, Quantum dots are core-shell nanocrystals. For biological studies, QDs are coated with an organic coating layer. B, Tunable light emission observed in semiconductor QDs. This image shows 10 distinguishable emission colors of ZnS-capped CdSe quantum dots excited with a near-UV lamp. From left to right (blue to red), the emission maxima are located at 443, 473, 481, 500, 518, 543, 565, 587, 610, and 655 nm.

dye signals. It is also possible to use multicolor QDs to simultaneously image several targets inside living cells or on the cell surface. This is especially useful in the early detection and identification of cancer tumors based on multiple markers [2].

Two key issues in utilizing QDs as fluorescent biological labels are (i) making high quality nanocrystals and (ii) choosing an appropriate surface coating technique that enables the nanocrystals to be water-soluble and functionalizable while avoiding deleterious effects on the optical properties [17,18]. To obtain robust and biocompatible QDs capable of long term stability in aqueous solution, strategies have been devised using direct adsorption of dihydrolipoic acid (DHLA) on the surface (leading to negative charges), and then electrostatic self-assembly to positively charged proteins [19,35]. Other strategies employ hydrophilic organic dendron ligands [36], and micellular encapsulation using phospholipids [17]. Importantly, amphiphilic polymer coated QDs conjugated to streptavidin have become commercially available [18]. A novel approach is based on the adsorption of bifunctional ligands such as mercaptoacetic acid, mercaptosuccinic acid, dithiothreitol, glutathione or histidine directly to the QD surface [37]. It has been shown that many mercapto compounds (e.g., mercapto-benzoic/propionic/undecanoic/decanoic acid) are amenable to this procedure [38,39]. A variation of this direct adsorption method is to incubate water soluble QDs with thiol-containing biomolecules, which slowly replace the surface mercapto ligands via mass action [40–42]. However, all these modifications result in several macromolecules being attached to one nanocrystal; as a result, the overall size is typically 15–20 nm, increased by 12–15 nm above the original nanocrystal.

Although QDs are very attractive fluorescence imaging probes for biological studies, there are challenges in using QD probes for intracellular imaging, including delivering QD probes into living cells, low signal-to-noise ratio, and the non-specific interaction between QDs and intracellular organelles. The size of QD probe, especially functionalized QDs may also be an issue when using QDs to study protein-protein interactions or the assembly of protein machines inside living cells due to potential interference. The development of QD bioconjugates of <5 nm remains a significant challenge.

1.2 Quantum dot-fluorescent protein FRET probes

QDs have been used in various FRET probes [43]. QDs make excellent FRET donors because of their exceptional brightness and high quantum yields [44–46], their capacity to bind multiple acceptor molecules [22], and the unique qualities of their characteristic excitation and emission spectra [45]. The broad excitation range of the QDs allows them to be excited far from the excitation range of the acceptor molecule, minimizing the background due to direct excitation of the acceptor, while the narrow and tunable QD emission peak can be optimally matched with the absorption spectrum of the desired acceptor. In addition, QDs with different sizes that emit in the visible range are best excited by UV light, allowing for color multiplexing [47]. Recent reports have described the approaches using QDs as a FRET donor with organic fluorophores, organic quenchers, or gold nanoparticles as the acceptor [30–32].

When commercially available QDs are used as donors for FRET studies, often the FRET acceptor is either covalently bound to the organic coating using standard cross-linking chemistry [30] or bound using a biotin-streptavidin interaction [31]. The biotin-streptavidin interaction is a technically simpler conjugation strategy, but results in large probe size and further increases the distance between the donor and acceptor molecules, thereby substantially reducing the FRET efficiency, since the FRET efficiency is inversely proportional to the distance between the donor and acceptor molecules to the sixth power [48]. As an alternative, polyhistidine peptide tags that utilize non-covalent, high affinity binding to metals have been developed and thoroughly characterized [22,32,49,50]. Since polyhistidine is able to chelate ions accessible in the ZnS capping layer of the most commonly used CdSe/ZnS core-shell QDs [50], the use of polyhistidine peptide tags in a QD-based FRET assay results in a much smaller distance between the donor and acceptor compared with other acceptor bioconjugation schemes. This strategy has been demonstrated for protein-QD conjugation when QDs are coated with dihydolipoic acid (DHLA); these QDs tend to aggregate under acidic conditions [51]. The polyhistidine peptide tag has been used with commercially-available QDs (QDots from Invitrogen) to demonstrate the utility of QDs as a bioluminescence resonance energy transfer (BRET) acceptor with luciferase as the donor [33]; however, in this case the histidine tag interacted with Ni^{2+} ions chelated by a high density of carboxyl groups in the organic coating, rather than binding directly to the inorganic QD surface. More recently, QD-fluorescent protein based FRET probes have been developed [43], based on polyhistidine coordination to the inorganic surface of commercially-available QDs, demonstrating that fluorescent proteins (FPs) are exceptional FRET acceptors for QD donors (Figure 2). The use of fluorescent proteins as acceptors has several benefits. For example, standard molecular biology techniques can easily be used to modify the FPs to include the polyhistidine tag, a variety of linkers between the protein bulk and the tag, and amino acid sequences that could contribute to the functionality of the QD-FRET probe, such as a cleavage sequence for a protease in order to produce a FRET-based probe to measure enzyme activity. Once a plasmid for the recombinant protein is designed, fluorescent proteins can be ex-

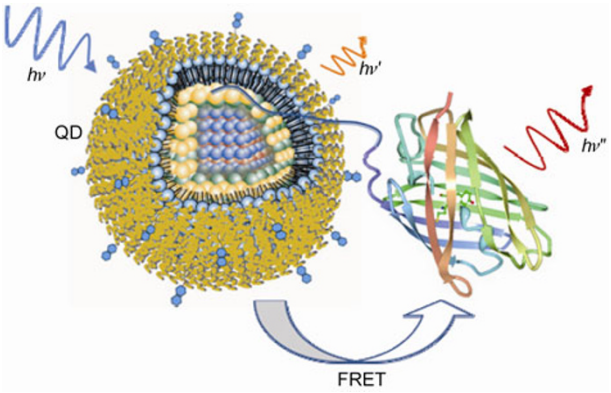

Figure 2 Schematic diagram of the FRET interaction between a quantum dot, specifically a T2-MP EviTag (Evident Technologies), and a GFP-like fluorescent protein. A polyhistidine sequence inserted at the N-terminus of the mCherry shown here coordinates to the ZnS capping layer of the QD, bringing the two into close proximity. Under excitation of the QD, energy is non-radiatively transferred to the fluorescent protein and sensitized emission is observed.

pressed in *E. coli* in large quantities, and the presence of the polyhistidine on his-tagged proteins facilitates protein purification using immobilized metal affinity chromatography (IMAC). The large variety of GFP-like fluorescent proteins now available with emission wavelengths spanning the entire visible range [52,53] also provides an array of possible fluorescent protein acceptors for QDs with different colors.

A specific application of the QD-FP FRET probes is the intracellular pH measurement in biological and disease studies. Intracellular pH (pH_i) plays a critical role in the physiological and pathophysiological processes of cells [54], and fluorescence imaging using pH-sensitive indicators can provide a powerful tool to assess the pH_i of intact cells and sub-cellular compartments. As shown in Figure 2, the QD-based ratiometric pH sensor, comprising a QD (as FRET donor) and pH-sensitive fluorescent proteins (FPs), exhibiting dramatically improved sensitivity and photostability compared to BCECF, the most widely used fluorescent dye for pH imaging. We found that Förster resonance energy transfer (FRET) between the QD and multiple FPs modulates the FP/QD emission ratio, exhibiting a >12-fold change between pH 6 and 8. The modularity of the probe enables customization to specific biological applications through genetic engineering of the FPs, as illustrated by the altered pH range of the probe through mutagenesis of the fluorescent protein. The QD-FP probes facilitated the visualization of the acidification of endosomes in living cells following polyarginine-mediated uptake. These probes have the potential to enjoy a wide range of intracellular pH-dependent imaging applications that are not feasible with fluorescent proteins or organic fluorophores alone, including tracking the endosomal release of nanocarriers for drug/gene delivery, as well as monitoring pH and/or metal ion concentration in both the intracellular and extracellular environment.

1.3 Molecular beacons

The ability to image specific ribonucleic acid (RNA) in living cells in real time can provide essential information on RNA synthesis, processing, transport, and localization. However, quantitative methods such as real-time polymerase chain reaction (PCR) and DNA microarrays rely on the use of cell lysates thus not able to obtain important spatial and temporal information. Fluorescent proteins and other reporter systems cannot image endogenous RNA in living cells. Fluorescence *in situ* hybridization (FISH) assays require washing to achieve specificity, therefore can only be used with fixed cells. Nanostructured probes for RNA detection in living cells have been developed; they promise to open new and exciting opportunities in sensitive gene detection for a wide range of biological and medical applications.

Of particular interest are molecular beacons, a class of ligonucleotide (ODN) hairpin probes that have been used for RNA imaging in living cells. As illustrated in Figure 3A, molecular beacons are single-stranded DNA or RNA molecules labeled at one end with a reporter fluorophore and at the other end with a quencher; they are designed to form a stem-loop hairpin structure in the absence of a complementary target so that fluorescence of the fluorophore is quenched. Hybridization with the target nucleic acid opens the hairpin and physically separates the fluorophore from quencher, allowing a fluorescence signal to be emitted upon excitation (Figure 3A). This enables a molecular beacon to function as a sensitive probe with a high signal-to-background ratio. Under optimal conditions, the fluorescence intensity of molecular beacons can increase by >200-fold upon binding to their targets [55]. The ability to transduce target recognition directly into a fluorescence signal with high signal-to-background ratio has allowed molecular beacons to enjoy a wide range of biological and biomedical applications, including real-time monitoring of PCR, genotyping and mutation detection, multiple analyte detection, assaying for nucleic acid cleavage in real-time, cancer cell detection, studying viral infection, and monitoring RNA expression and localization in living cells [56–70].

As illustrated in Figure 3A, a conventional molecular beacon has four essential components, a loop, stem, fluorophore, and quencher. The loop usually consists of 15–25 nucleotides and is selected to have a unique antisense targeting sequence. The stem, formed by two complementary short-arm sequences, is typically 4–6 bases long and chosen to be independent of the target sequence. The use of a single type of reporter dye on each molecular beacon allows multiple, optically distinct, molecular beacons to be visualized simultaneously (i.e., multiplexing) [56,61]. This important attribute could potentially be taken advantage of to highlight the orchestration between various gene expression patterns in living cells. In fact, several groups have already demonstrated the feasibility of simultaneously imaging multiple

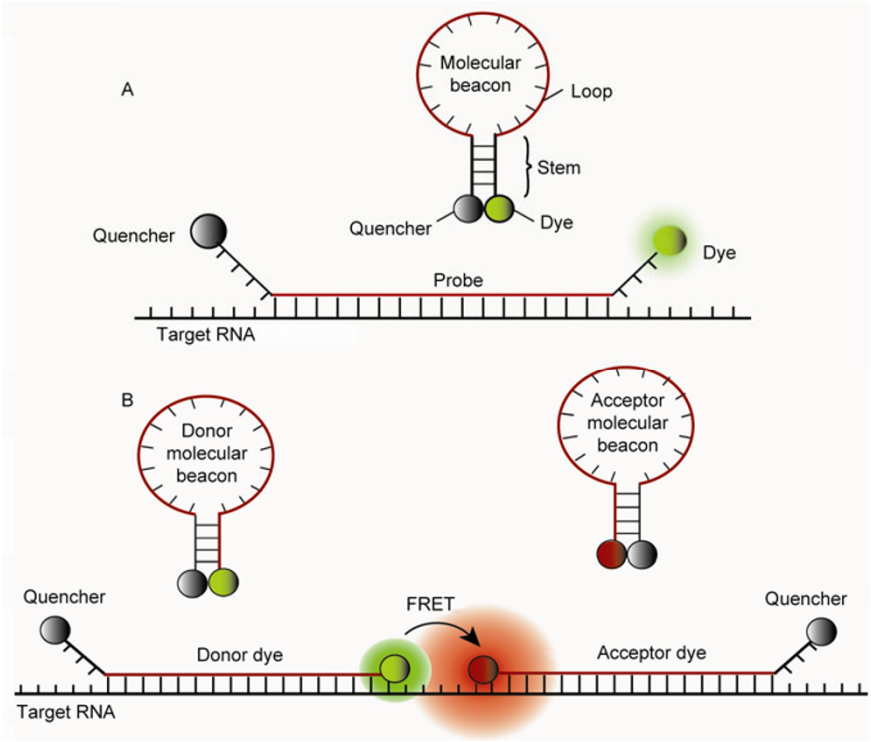

Figure 3 Illustrations of molecular beacons for live-cell RNA detection. A, Molecular beacons are dual-labeled stem-loop oligonucleotide hairpin probes with a reporter fluorophore at one end and a quencher molecule at the other end. B, Dual FRET donor and acceptor molecular beacons hybridize to adjacent regions on the same mRNA target resulting in FRET signal.

genes in single living cells with molecular beacons [69,70].

To further reduce background signal, especially that due to degradation of beacons by endonucleases in living cells, a novel dual FRET-molecular beacons approach was developed; it utilizes a pair of molecular beacons each labeled with a donor and acceptor fluorophore as illustrated in Figure 3B [65,66]. The probe sequences are chosen such that the molecular beacons hybridize to adjacent regions on a single nucleic acid target, similar to the dual FRET-linear probes. The resulting FRET signal (i.e., sensitized emission of the acceptor fluorophore) upon probe hybridization serves as a positive signal, which can be readily discerned from non-FRET false-positive signals due to probe degradation and nonspecific probe opening. Dual FRET-molecular beacons, therefore, combine the low-background signal and high specificity of molecular beacons with the ability of two-probe FRET assays to differentiate between true target recognition and false-positive signals. It has been demonstrated that upon hybridization to nucleic acid targets, dual FRET-molecular beacons can provide a better signal-to-background ratio than the single molecular beacon approach when appropriate FRET pairs are selected [65,66].

In the conventional molecular beacon design, the stem sequence is typically independent of the target sequence (Figure 3A); however, dual FRET molecular beacons can be designed such that all the bases of one arm of the stem (to which a fluorophore is conjugated) are complementary to the target sequence, thus participating in both stem formation and target hybridization (shared-stem molecular beacons) [71] (Figure 3B). The advantage of this shared-stem design is to help fix the position of the fluorophore that is attached to the stem arm, limiting its degree-of-freedom of motion, and increasing the fluorescence resonance energy transfer (FRET) in the dual FRET molecular beacon design.

Dual FRET molecular beacons have been used to detect K-Ras, surviving and oct4 mRNAs in HDF, Miapaca-2, and H1 cells, respectively [66,72]. Interestingly, k-Ras mRNAs seemed to localize with a filamentous pattern in HDF cell whereas survivin mRNAs seemed to localize in a non-symmetrical pattern within Miapaca-2 cells, often to one side of the nucleus of the cell. mRNA localization in living cells is believed to be closely related to post-transcriptional regulation of gene expression but much remains to be seen if such localization indeed targets a protein to its site of function by producing the protein ‘right on the spot’. Using a dual beacon approach, the transport and localization of Oskar mRNA in drosophila melanogaster oocytes has also been visualized [64]. In this work, molecular beacons with 2′-O-methyl backbone were delivered into cells using microinjection and the migration of Oskar mRNAs were tracked in real time, from the nurse cells where it is produced to the posterior cortex of the oocyte where it is localized. Clearly, the direct visualization of

specific mRNAs in living cells with molecular beacons will provide important insight into the intracellular trafficking and localization of RNA molecules.

One of the critical steps in the accurate detection of RNA molecules in living cells is the efficient delivery of molecular beacons into the cytoplasm. Oligonucleotide-based probes are generally prevented from gaining access to the cytoplasm due to the cell membrane [73]. Several methods have been developed to deliver molecular beacons into live cells include microinjection, electroporation, and the use of cell-penetrating peptides (CPP), steptolysin O (SLO) or polycationic molecules such as liposomes and dendrimers.

Streptolysin O (SLO), which is a pore-forming bacterial toxin, has been used as a simple and rapid means of introducing oligonucleotides into eukaryotic cells [74–76]. SLO binds to cholesterol molecules on cell surface and oligomerizes them into a ring-shaped structure to form pores of approximately 25–30 nm in diameter, allowing the influx of both ions and macromolecules. An essential feature of this technique is that the toxin-based permeabilization is reversible [77]. This can be achieved by introducing oligonucleotides with SLO under serum-free conditions and then removing the mixture and adding normal media with serum and calcium [75,77]. Since cholesterol composition varies with cell types, the permeabilization protocol needs to be optimized for each cell type by varying temperature, incubation time, cell number and SLO concentration.

A wide variety of cargos have been delivered to living cells both in cell culture and in tissue using cell penetrating peptides [78,79]. To deliver molecular beacons into cells, Tat peptides were conjugated to molecular beacons using different linkages (Figure 4A and B); the resulting peptide-linked molecular beacons were delivered into living cells to target GAPDH and survivin mRNAs [67]. At relatively low concentrations peptide-linked molecular beacons were internalized into living cells within 30 min with nearly 100% efficiency. Peptide-based delivery did not interfere with molecular beacon binding to survivin or GAPDH, since similar levels of fluorescence and a similar pattern of localization were seen in cells with beacons delivered using alternative means. Peptide-linked molecular beacons show impressive potential as an all-in-one molecule capable of self-delivery, targeting and reporting in live cells.

Peptide-linked molecular beacons can also be delivered using a SLO-based approach to target RNA molecules in the cell nucleus by attaching a nuclear localization signal (NLS) peptide to a molecular beacon. Molecular beacons designed to target small nuclear RNAs (snRNA) U1 and U2 were linked to NLS peptides and delivered to cells using the SLO based reversible membrane permeabilization method (Figure 4C). The small nucleolar RNA U3 was delivered into the nuclei of live HeLa cells, and the localization and co-localization (U1 and U2) of these nuclear RNAs was imaged [80]. This delivery method can potentially be used to image transcriptional and post-transcriptional processing of RNAs in the nucleus of living cells.

2 Nanoparticle-based MRI and MR/PET imaging contrast agents

Multimodality imaging combines two or more distinct im-

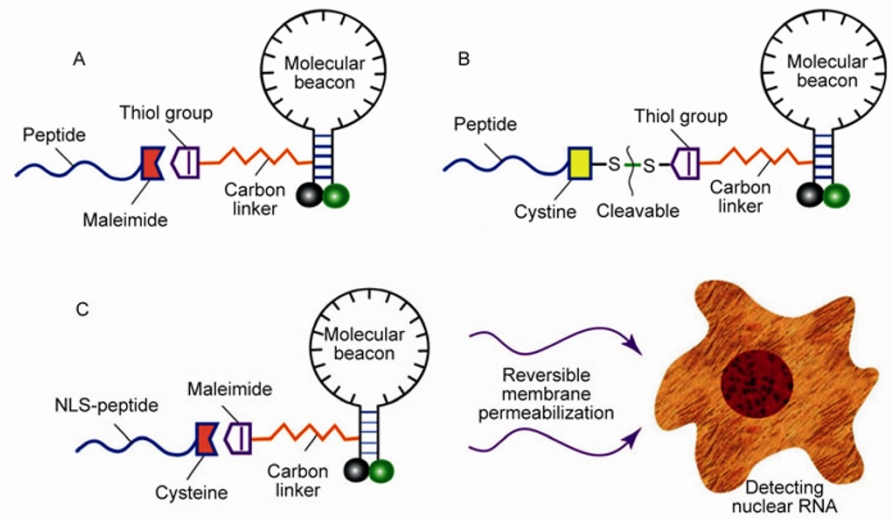

Figure 4 A schematic of peptide-linked molecular beacons. A, A peptide-linked molecular beacon using the thiol-maleimide linkage in which the quencher-arm of the molecular beacon stem is modified by adding a thiol group which can react with a maleimide group placed to the C terminus of the peptide to form a direct, stable linkage. B, A peptide-linked molecular beacon with a cleavable disulfide bridge in which the peptide is modified by adding a cysteine residue at the C terminus which forms a disulfide bridge with the thiol-modified molecular beacon. This disulfide bridge design allows the peptide to be cleaved from the molecular beacon by the reducing environment of the cytoplasm. C, A schematic illustration of the design of a peptide-linked molecular beacon and its delivery into cell nucleus. The NLS peptide is covalently linked to the molecular beacon using a modified nucleotide in its quencher arm. The NLS linked molecular beacons are delivered into the cytoplasm first using Streptolysin O (SLO), and the NLS peptide actively transports the probes into the nucleus of a living cell.

aging modalities in a way that leverages the respective strengths and weaknesses of each imaging technology. Examples include combined PET-CT [81], PET-MR [82,83] and MR-fluorescence imaging [84,85], which often generates results superior to both modalities operating separately. The combination of positron emission tomography (PET) with X-ray computed tomography (CT) has become the gold standard in oncologic imaging [81]. Positron emission tomography is the most sensitive human molecular imaging modality and produces whole body images of functional and molecular information. CT rapidly acquires whole-body images at high resolution but exposes patients and experimental animals to substantial doses of ionizing radiation. Magnetic resonance imaging (MRI), in comparison, uses no ionizing radiation and provides soft tissue contrast superior to CT. Combining PET with the high-resolution, spectroscopic, or contrast enhancement abilities of MRI would produce a breakthrough in the detection and monitoring of disease [82].

Nanoparticles possess unique characteristics that make them well suited as probes for molecular imaging [86]. Nanoparticles, including metal, metal oxide and semiconductor nanoparticles can be synthesized in a systematic fashion to have precise diameter with narrow size distributions. As particles become smaller, their surface area to volume ratio increases significantly. Engineering of nanoparticle surface chemistry allows the surface area to be decorated with therapeutic molecules, imaging agents, targeting ligands, or nucleic acids. To perform nanoparticle-based *in vivo* imaging of molecular markers associated with disease development, the nanoparticles must be functionalized with specific targeting ligands [87]. Distinct ligands and reporters can be attached to a single particle to allow multiplexing and multi-functionality. A single nanoparticle can be conjugated with a large number of targeting ligands, increasing the affinity of the nanoparticle to its biological target through a phenomenon known as multivalency. Additionally, a nanoparticle can be conjugated with a large number of reporter molecules (e.g., fluorophores, radionuclides), increasing signal-to-noise in imaging applications.

The unique qualities of nanoparticles described above make them superior in many ways to traditional low molecular weight MRI contrast agents and PET probes [88]. Compared to gadolinium-based MRI contrast agents, nanoparticle MRI contrast agents circulate in the blood for longer periods of time, offer greater sensitivity, and may produce fewer side-effects [89]. Radiolabeled nanoparticles can circulate for longer periods of time than small molecule PET tracers and can carry greater numbers of radionuclides [90]. Nanoparticles are therefore a promising platform for the construction of MRI and PET contrast agent for *in vivo* imaging.

The most promising nanoparticle system as contrast agent for multimodality *in vivo* imaging is superparamagnetic iron oxide nanoparticles (SPIOs) [91,92]. A variety of SPIOs with different cores and surface coating were synthesized, and several are currently under clinical trials for imaging liver tumors and metastatic lymph nodes [93–98]. A SPIO, in general, is composed of maghemite or magnetite crystals less than 20 nm in diameter. Unlike widely used paramagnetic gadolinium chelates, these nanocrystals contain thousands of Fe atoms and approach saturation magnetization under a magnetic field typical for MRI [99]. Each nanocrystal can generate signal contrast several orders of magnitude higher than a gadolinium chelate. In addition, iron oxide has little toxicity for *in vivo* applications. These features make SPIOs an appealing candidate for early detection and diagnosis of human diseases [96,100–102].

A novel nanoparticle-based dual-modality PET/MR imaging contrast agent consists of a SPIO core coated with PEGylated phospholipids and labeled with a radiotracer (^{64}Cu) [103], as shown in Figure 5A. To label SPIOs with positron-emitting ^{64}Cu, the chelator 1,4,7,10-tetraazacyclo-dodecane-1,4,7,10-tetraacetic acid (DOTA) was conjugated to PEG termini. The ^{64}Cu-SPIO probes produced strong MR and PET signals, and were stable in mouse serum for 24 h at 37°C. Biodistribution and *in vivo* PET/CT imaging studies of the probes showed a circulation half-life of 143 min, and high initial blood retention with moderate liver uptake, making them an attractive contrast agent for disease studies.

For an imaging modality with specific design characteristics, the performance of *in vivo* imaging is determined by signal-to-noise ratio and detection sensitivity; nanoparticle-based contrast agent can improve both. It is critical to synthesize SPIOs with substantial signal enhancement on a per-particle basis to improve sensitivity, and to tailor nanoparticle surface chemistry to optimize the specific accumulation (attachment) of SIPOs in diseased cells, tissues or organs. There are two major factors in determining the signal enhancement generated by the SPIOs: iron oxide core (size and material) and the coating (thickness and chemical composition). SPIOs can induce an increased T_2 relaxivity in MRI, which is determined by the translational diffusion of water molecules in the inhomogeneous magnetic field surrounding the SPIO [104–106]. It has been established that T_2 relaxivity of SPIOs increases with the magnetization and the size of iron oxide cores if the total amount of iron is constant [104,107]. The magnetization of SPIOs can be enhanced by using cores formed by elementary iron or by doping iron oxide with other magnetic elements such as nickel, cobalt and manganese [96,108,109]. Further, the core size of SPIOs can be increased by employing controllable crystallization through thermo-decomposition of iron complex in organic solvents [94,95,109,110].

To date, many nanocrystals are initially prepared as a colloid stabilized by hydrophobic surfactants in nonpolar solvents. For example, iron oxide nanoparticles and quantum dots can be synthesized by thermal decomposition of precursor compounds in organic solvents [94,111,112].

These methods facilitate size tuning and improve the size distribution of nanocrystals. However, as-synthesized nanoparticles will aggregate in aqueous buffers unless protected by hydrophilic molecules. In order to disperse in aqueous solutions and be functionalized, the iron oxide core needs to be coated with either natural macromolecules or synthetic polymers [94,98,113]. Although the physical functionality of a nanoparticle is mainly attributable to its crystalline core, the coating plays an indispensible role in the biomedical applications. The coating layer must render nanoparticles water-dispersible, prevent aggregation, reduce non-specific adsorption in biological systems, and provide a platform for conjugation of targeting ligands or other functionalities. The size, charge, hydrophilicity and flexibility of the coating molecules are critical mediators for the *in vitro* and *in vivo* performance of nanoparticles [109,114,115]. For example, the coating molecules of a SPIO can exclude water from its surface, hinder water diffusion, or immobilize nearby water molecules by forming hydrogen bonds, all may affect the nuclear relaxation of water protons. SPIOs synthesized with distinct coating schemes can exhibit significantly different T_2 relaxivity even if their iron oxide core sizes are similar. Furthermore, the density and class of reactive groups on the nanoparticle surface are not only important for conjugation chemistry but also regulate the interactions between nanoparticles and their targets [116–118].

Amphiphilic surfactants can be adsorbed to the surface of hydrophobic nanoparticles with the hydrophilic portion of the surfactants exposed to the aqueous solution. The adsorption is driven by hydrophobic interactions between the amphiphilic surfactants and the nanoparticle surface. Amphiphilic polymers with a low critical micelle concentration (CMC), e.g., Poloxamer®, Poloxamine® and lipid-PEG copolymer, can form a stable coating layer around hydrophobic cores [98,114,119]. Amphiphilic polymer coated carbon nanotubes, polystyrene beads, quantum dots, and superparamagnetic iron oxide nanoparticles have been used in *in vitro* and *in vivo* applications [17,97,98,114,120,121]. This coating can be generalized for many hydrophobic nanocrystals because it does not rely on the reactivity of the crystal surface [98]. This method can also be used to produce multifunctional nanoparticles by adding functionalized polymers to the initial coating mixture, making it an attractive approach for coating nanocrystals with hydrophobic surfaces [122].

Hydrophobic nanocrystals are usually encapsulated with amphiphilic polymers through a film hydration process [17,97,122,123]. In this method, amphiphilic polymers and nanocrystals are first distributed in a thin film, which is often performed by dispersing all components in chloroform and evaporating the solvent with a rotary evaporator, resulting in a film with uniformly distributed components. The components can assemble into water-dispersible nanoparticles when the film is hydrated in an aqueous buffer. This process usually requires energy input from intensive heating and sonication. The coating formation depends on the polymer concentration, ionic strength, pH value and temperature [124,125]. Despite its broad usage, the film hydration procedure is hindered by two competing processes: formation of empty micelles by the coating polymers alone and aggregation of nanocrystals. The aggregation of nanocrystals is nearly irreversible due to their high surface energy. To avoid aggregation, it is crucial to separate the individual nanocrystals with the coating polymers in the thin film. A common approach is to increase the ratio between the coating polymers and nanocrystals in the initial mixture. However, it is difficult to achieve a good separation of nanocrystals using the film hydration method, and the coated nanoparticles are often accompanied by a large amount of empty micelles and aggregated nanocrystals. In addition, certain functional groups, e.g., maleimide, can hydrolyze readily in aqueous buffers once heated, thus incompatible with the film hydration method.

Recently, a dual solvent exchange method was developed for forming water-dispersible nanoparticles with a small amount of amphiphilic polymers [126]. In this method, the abrupt phase transition (from a solid film to a solution) in film hydration is replaced with a mild solvent exchange procedure performed entirely in solution. Specifically, DMSO, which is miscible with chloroform and water, is used to bridge the gap between the two solvents. Compared with the conventional film hydration method, this new method requires less work on purification, leads to much improved coating efficiency and quality, and can be readily adopted for large-scale coating of a broad range of nanocrystals. This method also provides a means to control the density of coating molecules and reactive groups on the nanoparticle surface. In particular, the amount of initial amphiphilic polymer required for effective nanoparticle coating is one to two orders of magnitude lower than those reported in the literature, which minimizes the formation of empty micelles. The dual solvent exchange method facilitates a uniform and controllable surface modification of nanoparticles with variable surface density of DSPE-PEG and functional groups, which may reduce non-specific interaction with proteins, achieve desirable in vivo biodistribution of nanoparticles, and significantly enhance the ability of nanoparticles to target specific disease markers.

To demonstrate the ability of detecting early-stage tumor using SPIOs as a contrast agent in MRI, animal studies of *in vivo* tumor imaging were performed with DSPE-PEG coated SPIOs [115], which exhibited longer blood circulation half-life (23.2 min) compared with other nanoparticles coated with DSPE-mPEG1000. Tumors were induced by implanting human U87 glioblastoma cells subcutaneously in nude mice. After the tumors reached 3–5 mm in diameter, the tumor-bearing mice were examined with a 7T MRI scanner before and one hour after tail vein injection of SPI-

Os conjugated with antibodies against mouse VEGF receptor-1. The specificity of VEGFR-1-targeting SPIOs was confirmed using an *in vitro* assay. As shown in Figure 6, injection of the 14 nm SPIOs resulted in a significant enhancement in T_2 contrast of the tumor tissue.

Although nanoparticle-based contrast agents for MRI or combined MR/PET imaging have a great potential, there are also significant challenges in translating the nanotechnology into clinical use. Clearly, the nanoparticle probes must have good biocompatibility and minimal toxicity [127]. The clearance of nanoparticles from the body, if they are not biodegradable, is a very important aspect. It is also essential to have a sufficient accumulation of nanoparticles inside (or on the surface) of diseased cells, tissues (such as tumor) or organs in order to generate a high enough signal-to-noise ratio in disease detection. Achieving a good balance among sensitivity, signal-to-noise ratio and safety, the size, functionalization (the type and amount of targeting ligand), surface chemistry (coating, reporters) and the total amount of contrast agent delivered need to be optimized.

3 Nanoparticle-based CT contrast agents

X-ray computed tomography (CT) is one of the most widely used imaging modalities in diagnostic medicine due to the cost effectiveness, deep tissue penetration, and high resolution [128]. CT contrast agents are typically iodine or barium compounds, which are usually used for intravascular and gastro-intestina imaging, respectively. Currently, small iodinated molecules are routinely used for *in vivo* contrast enhancement in the clinical setting, since iodine has a high X-ray absorption coefficient among nonmetal atoms. However, short circulation half-life, non-specific distribution, and potential renal toxicity have limited their imaging and targeting performance *in vivo* [129]. Liposomes with entrapped iodinated molecules are effective contrast agents due to their prolonged circulation half-time [130]. In one study, nodules showed significantly higher signal enhancement even on day 3 and day 7 after tail vein injection of liposomal-Iodinated contrast agent [131]. There have also been studies focusing on iopromide-containing lipid vesi-

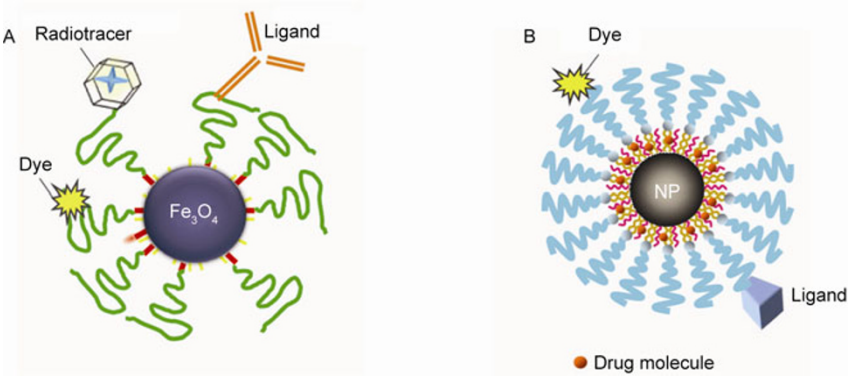

Figure 5 Nanoparticle-based contrast agents *in vivo* imaging and drug/gene carriers for *in vivo* delivery. A, Iron oxide magnetic nanoparticle probes for MRI and combined MR/PET medical imaging. B, Nanocarriers for targeted drug/gene delivery in disease treatment.

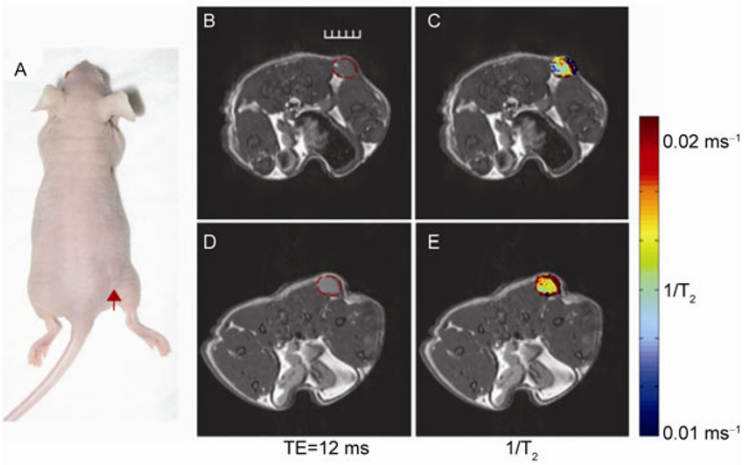

Figure 6 SPIO based *in vivo* tumor imaging. MRI experiments were performed using spin-echo sequence. A, Arrow shows the location of the subcutaneous tumor. B and C, MR images of tumor before probe injection. D and E, MR images collected after 1 h following the injection of 14 nm SPIOs conjugated with antibodies against mouse VEGFR-1. Red dotted lines in B and D outline the tumor. Scale bar, 5 mm.

cles for CT imaging of liver tumor, which has progressed to the clinical trials [132]. However, It is necessary to have a very high total iodine dose to achieve significant contrast enhancement, and the associated high lipid concentrations raise a significant concern of the toxicity and clearance of liposomal CT contrast agent.

Over the past decade or so, nanoparticle based CT contrast agents that comprise high atomic number (high-Z) metal elements (such as gold, silver, bismuth, and tantalum) have emerged to overcome the shortcomings of iodine agents. Clearly, an optimal nanoparticle CT contrast agent should have high X-ray attenuation coefficient, low toxicity and cost, and small size. Since gold has a higher atomic number and X-ray absorption coefficient than iodine, gold nanoparticles (GNPs) have been developed as a CT contrast agent in recent years. Measurement of the X-ray absorption coefficient *in vitro* revealed that the attenuation of polyethylene glycol (PEG) coated GNPs (30 nm in diameter) is 5.7 times higher than that of the current iodine-based CT contrast agent. These GNPs also had a much longer blood circulation half-life than clinically used CT contrast agent (<10 min) [133]. Dendrimer-entrapped gold nanoparticles (Au DENPs) have also been developed as a molecular probe for CT imaging. Compared with traditional iohexol, the vascular system and the urinary system could be clearly imaged after 20 and 60 min injection respectively of Au DENPs into the tail vein [134].

Owing to the fact that silver nanoparticles (Ag NPs) have structural and crystalline similarity to gold nanoparticles, Ag NPs with tunable sizes can also be used for CT imaging. Dendrimer-stabilized silver nanoparticles (Ag DSNPs) with a diameter of 16.1 nm displayed an X-ray attenuation intensity close to that of a clinically used iodine-based contrast agent (Omnipaque) at the same molar concentration of the active element (Ag versus iodine), although the atomic number of Ag is lower than that of iodine, suggesting that Ag DSNPs have a great potential to be used as a CT imaging contrast agent [135].

Ever since noble metal nanoparticles were developed as X-ray contrast agents, researchers have been actively seeking alternative nanoparticle-based imaging probes that are not expensive for clinical use. Polymer-coated Bi_2S_3 nanoparticles were recently reported as an injectable CT contrast agent for enhanced *in vivo* imaging of the vasculature, liver and lymph nodes in mice [136]. With more than a five-fold increase in X-ray absorption than iodine, long circulation half-life *in vivo*, and an efficacy/safety profile comparable to or better than iodinated contrast agents, these nanoparticles and their bioconjugates may potentially be used for clinical CT imaging [137] (Figure 7). Targeted peptide (LyP-1) conjugated on the surface of Bi_2S_3 nanoparticles increased the homing efficacy of nanoparticles to breast tumor [138], suggesting that Bi_2S_3 nanoparticles can be developed as a targeting contrast agent for CT molecular imaging.

Tantalum is another strong candidate as a CT contrast agent due to its high X-ray attenuation coefficient, bioinertness and low cost. Tantalum oxide (TaO_x) nanoparticles

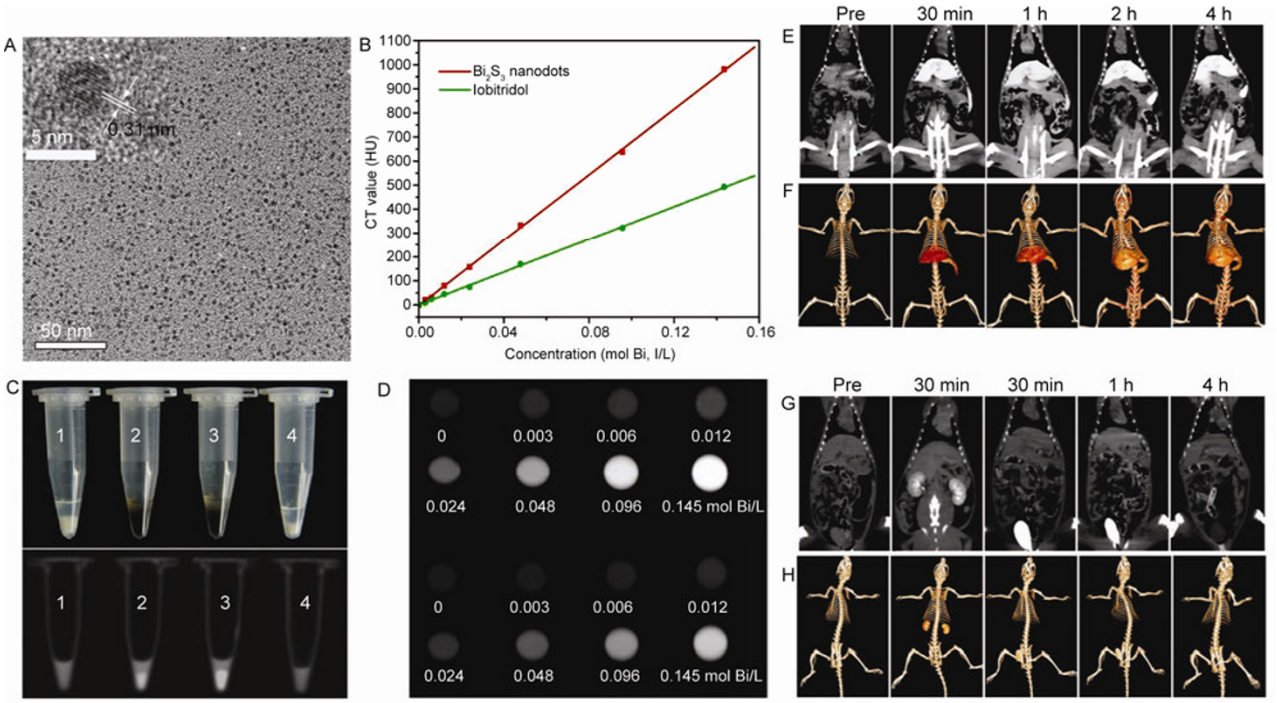

Figure 7 Bi_2S_3 nanoparticles as CT contrast agent. A, TEM image of Bi_2S_3 nanoparticles. B, CT value (HU) of PVP-coated Bi_2S_3 nanoparticles/Iobitridol as function of the concentration. C, Cell uptake analysis: bright field images (top) and CT images (bottom) of HeLa cells incubated with PVP-coated Bi_2S_3 nanoparticles and Iobitridol and without contrast agent for 24 h. D, *In vitro* CT images of PVP-coated Bi_2S_3 nanoparticles and Iobitridol with different concentrations. E and F, *In vivo* X-ray CT imaging of PVP-coated Bi_2S_3 nanoparticles. G and H, *In vivo* X-ray CT imaging of Iobitridol [137].

exhibited remarkable performances in *in vivo* X-ray CT angiography and bimodal image-guided lymph node mapping [139]. Most importantly, TaO_x nanoparticles can be easily functionalized with various biomolecules for tissue-specific uptake and multimodal imaging applications [140].

4 Nanoparticles for combined imaging and therapy

In cancer chemotherapies and gene therapies, the success of treatment relies on efficient delivery of therapeutics to the tumor. Although passive and active targeting can be explored to improve the efficacy of drug delivery, it is well recognized that solid tumors are highly heterogeneous in terms of vessel density, vascular permeability and interstitial compositions [141]. Drug distribution in the tumor may change considerably with the tumor type, stage and location. It is therefore critical to optimize drug/gene treatment for individual patients. The field of image guided drug delivery addresses this issue by utilizing imaging methods to monitor, guide and evaluate targeted delivery of therapeutics to tumor tissues. To avoid variations in the pharmacokinetics of imaging contrast agents and drug delivery vehicles, it is desirable to combine imaging and therapeutic functions to the same agent, which is often referred to as a theranostic agent.

With only a few exceptions, theranostic agents are developed using nanoparticle platforms. Over the past decade or so, nanoparticles with unique optical, magnetic and plasmonic properties have been extensively studied as contrast agents for different imaging modalities. Recent advances in nanofabrication further provide nanoparticles with rich physical and chemical properties that facilitate the incorporation of small molecular moieties. Multiple functionalities can be readily integrated to the same nanoparticle by modulating its structural and/or chemical compositions. A typical theranostic nanoparticle may have part or all of the following components: (i) imaging contrast agents, (ii) chemical bonds or physical interactions for loading and releasing of drugs and genes, (iii) targeting ligands, and (iv) elements that respond to external triggers such as ultrasound, light and magnetic field. Summarized in Table 1 are some of the functionalities that have been integrated using theranostic nanoparticles. While numerous combinations of these functionalities have been achieved, due to space limitations, only a few examples are covered in this review.

Imaging guided drug delivery can be performed by combining nanoparticles with distinct functions. For example, tumor targeting, imaging and drug delivery were performed with sequentially administrated gold nanorods, iron oxide nanoworms and drug loaded liposomes [142]. Gold nanorods bound to tumor vessels converted electromagnetic energy into heat, which triggered a blood coagulation cascades. This in turn led to enhanced accumulation of magnetic iron oxide nanoparticles or drug loaded liposomes that target fabrin and the coagulation transglutaminase FXIII. As the same time, thermographic imaging and fluorescence imaging were applied to examine the heating of gold nanorods and the tumor accumulation of iron oxide nanoparticles.

Magnetic iron oxide nanoparticles are the most well studied theranostic nanoparticles owing to their excellent biocompatibility [143], superior MRI T_2 contrast [115], magneto-mobility [144] and capability to be heated with an alternating magnetic field (Figure 5B) [145]. In the past few years, many forms of iron oxide nanoparticle based drug carriers have been developed by encapsulating iron oxide nanocrystals with various surface coating. It has been shown that mitoxantrone conjugated to starch coated SPIOs could effectively treat VX-2 squamous cell carcinoma in a rabbit model [146]. In this study, the SPIOs administrated intra-arterially were retained at the tumor site by an electromagnet, thus significantly reducing systemic toxicity. However, drug loading via chemical conjugation is restricted to a small group of drug molecules with reactive moieties. In contrast, iron oxide nanocrystals with micellar coating have great promise as carriers for many small chemotherapeutic drug molecules [147–150]. In micellar nanoparticles, iron oxide nanocrystals are synthesized with nonpolar capping molecules. Water-dispersible nanoparticles are obtained by coating the nanocrystals with a monolayer of amphiphilic copolymers through hydrophobic interactions [119,126]. Small hydrophobic molecules such as doxorubicin and paclitaxel can be stored in the hydrophobic core of micellar nanoparticles. The nanoparticles with amphiphilic capping molecules covalently bound to iron oxide surface can also adsorb drug molecules by hydrophobic interactions [151,152]. Another coating with broad drug loading capability is mesoporous silica [153]. Mesoporous silica coated magnetite exhibits excellent T_2 relaxivity and tumor imaging potentials. Small drug molecules and fluorophores can be loaded into the porous silica shell through either chemical conjugation or electrostatic interactions. Drug loading by hydrophobic or electrostatic interactions often affords much higher loading capacity than that of chemical conjugation. Nevertheless, drug molecules may be prematurely released from the nanoparticles in systemic circulation. To what extent the MRI signal of nanoparticles can predict the bio-distribution of drug molecules requires careful examination. Other major types of magnetic delivery vehicles include liposomes or cerasomes containing iron oxide nanocrystals. Magnetic liposomes containing doxorubicin accumulated in tumors under the influence of a magnetic field and significantly suppressed tumor growth [154].

Magnetic iron oxide nanoparticles have also been used as the carriers for *in vivo* gene delivery. The iron oxide cores provide MRI signal contrast and magneto-mobility. Multifunctional nanoparticles were constructed by simultaneously conjugating siRNA, near infrared fluorophores (Cy5.5)

Table 1 Functionalities of theranostic nanoparticles

Imaging modalities	Drug/gene loading mechanisms	Other functionalities
MRI (SPIOs, MnO, Gd^{3+}) [147−153,155−157,160−162] CT (gold nanoparticles, iohexol liposomes) [163] Fluorescence imaging (quantum dots, upconversion nanocrystals and organic fluorophores) [147,152,153,164,165] PET (^{64}Cu) [159] SPECT (^{111}In, ^{99m}Tc, ^{123}I and ^{131}I) Thermoaccoustic imaging (gold nanorods and gold nanocages)	Chemical conjugation [155,156,160,166] Encapsulation (liposomes) [154] Hydrophobic interaction (micelles and nanoparticles coated with amphiphilic polymers) [147−150] Electrostatic interaction (positively charged liposomes, polymers and mesoporous silica) [144,159]	Degradability (pH sensitive, enzyme cleavable, and reducible bonds) [160,166] Heat generation (infrared laser, alternating magnetic field and ultrasound) [145,165] Magneto-mobility (magnetic nanoparticles) [144,167,168] Photosensitizer [162]

and cell membrane translocation peptides to dextran coated iron oxide nanoparticles [155]. Tumor accumulation of the nanoparticles was confirmed with both MRI T_2 imaging and fluorescence imaging and was in good agreement with the knockdown effects of siRNAs. In a similar preparation, siRNA, Cy5 and RGD peptides were conjugated to the surface of $MnFe_2O_4$ nanoparticles that possess high T_2 relaxivity [156]. Magnetic liposomes that bound siRNAs by electrostatic interactions were also developed, which inhibited tumor angiogenesis and proliferation by suppressing the expression of EGF receptor in a mouse tumor model [144].

Iron oxide nanoparticles can only provide dark contrast in MRI, which is difficult for quantitative determination of the nanoparticle concentration. In contrast, nanoparticles conjugated with Mn^{2+} or Gd^{3+} chelates are capable of generating a bright signal in T_1-weighted MRI images. Such nanoparticles include micelles, polymeric particles and liposomes. However, most T_1 contrast agents have poor relaxivity compared with the T_2 relaxivity of iron oxide nanoparticles. Recently, hollow MnO nanoparticles were developed as a dual T_1 and T_2 contrast agent [157]. Core-shell T_1-T_2 dual mode nanoparticles that combined both $MnFe_2O_4$ and gadolinium were also synthesized [158]. It was showed that by separating gadolinium and $MnFe_2O_4$ with a silica oxide layer, the nanoparticles achieved both high T_1 and T_2 relaxivity. Performing both T_1- and T_2-weighted imaging could help exclude faulty signals and enhance diagnostic accuracy.

PET and SPECT (single-photon emission computed tomography) are being actively investigated for tumor detection. Both imaging techniques have excellent detection sensitivity but offer no anatomical information. The two imaging techniques are often combined with CT or MRI in order to locate the site of the signal. PET and SPECT utilize radioisotopes such as ^{64}Cu, ^{111}In and ^{99m}Tc, the chelates of which can be conjugated to nanoparticles similar to that of Gd^{3+}. For example, ^{64}Cu-DOTA was linked to siRNA, which is in turn conjugated to transferrin targeted polycation nanoparticles for combined cancer imaging and treatment [159]. The bio-distribution of the nanoparticles was readily obtained in overlaid CT/PET images.

5 Engineered molecular machines for disease treatment

One of the most important areas of nanomedicine is the development of novel engineered molecular machines that possess the ability to quantify, control and manipulate biological functions in living cells in order to treat or prevent diseases. At the nanometer scale, these molecular machines are typically multi-component and multi-functional, with target recognition, actuation, manipulation, self-assembly and disassembly functions. Compared with simpler nano-scale devices, such as nanoparticle-based targeted drug/gene delivery vehicles and imaging contrast agents, molecular machines perform highly specific manipulation (such as DNA cutting) of biomolecular complexes in/on a living cell, therefore have much more demanding design requirements.

To date, the most promising molecular machines for nanomedicine applications are custom designed nucleases, which have become a valuable tool for specifically cleaving genomic sequences [169]. As shown in Figure 8, the primary forms of targetable nucleases are zinc finger nucleases (ZFNs) and transcription activator-like effector nucleases (TALENs) [170,171], each consists a DNA binding domain (zinc finger or Tal effector) fused to the Fok I non-specific DNA cleavage domain. These nucleases can be designed to create a DNA double-strand break (DSB) in a specific (pre-determined) target sequence, which can be repaired by the cellular DNA repair machinery. The primary means of re-ligation is error-prone non-homologous end joining (NHEJ). If a donor DNA template is supplied along with the nucleases, the break can be repaired using the homologous recombination (HR) pathway. This process can lead to genome editing of the endogenous gene if the donor sequence is mutated, has deletions, or contains additional sequences. Alternatively, HR trigger by ZFN or TALEN induced DSB can correct mutations of a gene that cause disease. Nuclease-induced DSB near the mutation can greatly increases the rate of HR [172], incorporating the supplied donor template, thereby enabling isolation of modified genes. The high efficiency of genome editing has greatly enhanced the capability to edit genomic sequences for basic research as

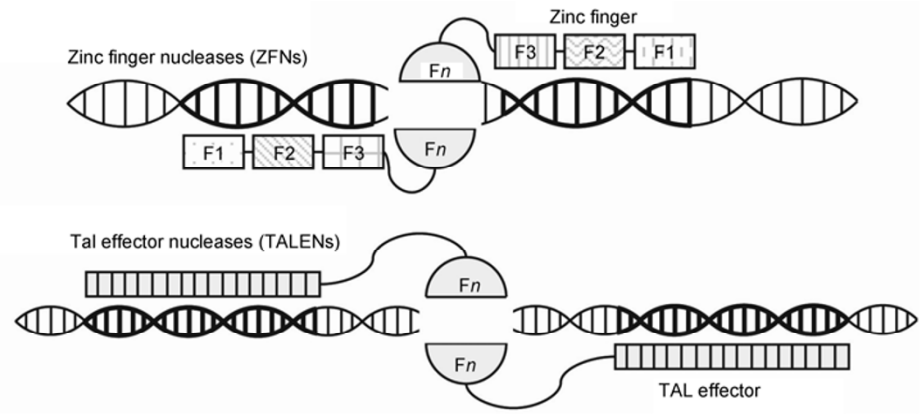

Figure 8 Engineered nucleases for gene targeting. Zinc finger nucleases (ZFNs) formed by coupling zinc finger proteins to Fok I nuclease domains can bind to a targeted DNA sequence and cut the DNA. Each zinc finger binds to 3 DNA bases, so a pair of 3-finger ZFNs can recognize an 18 bp DNA sequence. A transcription activator-like effector nuclease (TALEN) is formed by biding the Fok I nuclease domain to a transcription activator-like effector (TALE) consisting of an array of tandem repeats that mediate DNA recognition. Each repeat sequence contains a RVD (repeat variable di-residue) that determines base preference. A pair of nucleases (ZFNs or TALENs) are required to generate a double strand break or a nick on the DNA.

well as medical applications.

The specificity of ZFNs and TALENs is greatly increased by the need for a pair of nucleases, each binds one of the two target half-sites with correct orientation and spacing, resulting in Fok I dimerization and cleavage of the intervening DNA [173,174] (Figure 8). The DNA binding domains can either be Zinc Finger Proteins for ZFNs or transcription activator-like effector domains for TALENs. ZFNs have been in use for years and have been used extensively to modify the genomes of multiple model organisms and human cells. Their use has been limited by the difficulty in their rational design, which is greatly hindered by the importance of context on binding specificity. TALEN design is greatly simplified due to the straightforward relationship between the proteins sequence and binding specificity. The specificity of TALEN comes from a pair of amino acids within the ~34 amino acid repeats, the 'repeat-variable di-residues' (RVDs) [170,175].

The successful application of custom designed, engineered nucleases for treating human diseases requires identification of the possible off-target cleavage evens. The cleavage of nucleases at sites besides their target site is commonly referred to as off-target sites, and can lead to mutations, deletions or chromosomal changes. At this point there have been limited studies on off-target cleavage, but both ZFNs and TALENs have been found to have off-target cleavage, as identified by detecting NHEJ directed mis-repair at putative sites identified through similarity to the target sequence [176], or through methods monitoring DNA breaks or cytotoxicity.

Several methods have been introduced to improve the specificity of pairs of custom nucleases. The first is the modification of the Fok I domains to require that dimerization is only accomplished with one "left" and one "right" nuclease [177]. Another method uses a mutation that renders one of the two nucleases catalytically inactive, resulting in a single stranded break, though with decreased activity [178].

There are many potential medical applications of engineered nucleases, including the establishment of HIV-1 resistance in $CD4^+$ T cells by genome editing [179], and correcting genetic defects (including mutations, deletions or insertions) in treating single-gene disorders. An example is ZFN/TALEN based treatment of sickle cell disease (SCD) that caused by a single (A-T) mutation in the beta-globin gene. SCD is a painful and life shortening disease and afflicts primarily persons of African origin [180]. To use engineered nuclease to treat SCD, it will be necessary to design and optimize ZFNs or TALENs that bind specifically to the beta-globin gene, deliver them as well as wild-type donor templates into the nuclei of hematopoietic stem and progenitor cells (HSPCs) to induce a DSB or a nick at a preselected site near the beta-globin locus, shepherding the broken DNA ends into the homologous recombination (HR) pathway for gene correction. The autologous gene-corrected HSPCs can then be re-engrafted in the SCD patient to produce healthy red blood cells and replace sickle cells. HSPCs are the normal precursors of all blood cells, including the oxygen-carrying erythrocytes rendered dysfunctional in sickle cell patients. These cells are relatively rare in the body, but possess potent regenerative potential in that transplantation of a small amount of HSPCs is sufficient to rebuild the entire blood system of an organism. Thus, by isolating HSPCs that carry the sickle mutation, correcting this mutation *ex vivo*, and then transplanting the gene-corrected HSPCs back into affected recipients, it will be possible to provide enduring replacement of the blood-producing cells of SCD patients with unaffected precursors, thereby supplying healthy red blood cells and effectively curing the disease.

Although the gene correction approach for treating SCD rests on established scientific principles without any con-

ceptual barrier to its implementation, there are many practical and technological challenges in translating the nuclease-based gene correction approach to clinical practice. These include shifting repair pathway choice from NHEJ toward HR, increasing the spontaneous rate of gene correction by many orders of magnitude, identifying and minimizing unwanted off-targeting effects and gene rearrangements, and establishing a high-throughput, high efficiency delivery capability. These challenges can be overcome by optimizing nuclease and donor template designs, exploring alternative delivery methods, and applying novel imaging probes and methods to observe and systematically optimize each step in the gene correction process. It is likely that the methods and technologies developed in nuclease based SCD treatment can be applied to treating other diseases. It has been estimated that there are ~10000 human single-gene disorders, which impose a significant burden on human health worldwide. Therefore, the development of nanomedicine approaches for treating single-gene disorders based on engineered nucleases may have a significant impact to human health.

6 Opportunities and challenges in nanomedicine

Nanomedicine research and development that utilize nano-scale (1–100 nm) features of materials and structures at atomic, molecular and macromolecular levels have the potential to provide fundamental understanding of biological processes in living cells that would be otherwise unthinkable, establish the ability to precisely measure, control and manipulate the functions of biomolecules *in vivo*, and create medical reagents, devices and systems that have novel properties and functions because of their nano-scale features. For example, the diagnosis and treatment of atherosclerosis represents an area where targeted nanoparticles have great potential for noninvasive diagnosis, targeted therapy, and plaque stabilization. Specifically, it is possible to have nano-scale multifunctional devices that could detect thrombotic events *in vivo* and deliver therapeutic agents such as anticoagulants as needed. Therapeutic nanoparticles have the potential for curing inflammatory lung diseases, including biodegradable nano- and microparticles releasing anti-oxidant and anti-inflammatory drug molecules, and nanoparticles capable of sensing alveolar function and releasing drugs only when needed, restricting drug delivery to affected areas in heterogeneous disease conditions. Nanomedicine approaches may enable early detection of cancer, and the targeted delivery of anti-cancer drugs into tumor tissue, dramatically increasing their efficacy and decreasing the side effects. Nanoparticle (NP) based imaging probes may enable us to detect cancer stem cells and reveal the interaction between normal and cancer cells during the earliest stages of the cancer development, thus having the potential to eliminate death and suffering from cancer.

To successfully develop nanomedicine as a new field, there are significant challenges in achieving high efficacy and safety, and in technology translation and commercialization. Some of the major challenges in these areas are summarized in Table 2. Clearly, for nanomedicine to generate a large clinical impact, it has to produce methods, devices, drugs, procedures, tools or reagents that are better than existing counterparts, such as simpler, faster, cheaper or safer; more sensitive, specific or robust; or having entirely new functionalities. Achieving these will require concerted efforts by researchers in nano-science, nano-engineering, biology, chemistry, medicine as well as experts in manufacturing, commercialization, regulation, safety, and environmental protection.

To effectively develop nanomedicine, we must take a systems approach in addressing the major challenges. For example, for nanoparticles as an *in vivo* imaging contrast agent, the size and surface chemistry of nanoparticles need to be tailored to achieve optimal sensitivity, signal-to-noise, biodistribution, and the amount required in a well-balanced fashion. Similarly, for nanoparticle-based *in vivo* drug/gene delivery, the nano-carriers need to be well designed to achieve adequate cargo loading, controlled release, specific organ/cell internalization and accumulation, and quick clearance/degradation of the nanoparticles. For disease treatment using engineered nucleases, it is necessary to optimize the design of ZFNs or TALENs so that both high gene correction efficiency and minimal off-target effect can be realized. Most of the nanomedicine approaches involve cellular and/or *in vivo* delivery of nanoparticles, proteins,

Table 2 Major challenges in nanomedicine

Efficacy	Safety	Translation	Commercialization
Quality of NP synthesis & functionalization	Cytotoxicity	Impact to medicine	Scale-up
Sensitivity & specificity	Biocompatibility	Imaging probes & contrast agents	Barriers in regulation
Signal-to-noise	NP clearance	Targeted delivery vehicles	Robustness
Tunable blood circulation half-life	NP degradation	Molecular devices	Cost
Optimal biodistribution	Off-target effects	NP based drugs	Stability & storage life
Efficiency & throughput	FDA approval	Disease diagnosis, treatment & intervention	Quality control & BMP
Controllability & tunability	Environmental effects	Tissue repair/regeneration	Standardization
Optimal size & surface chemistry		Theranostics	Packaging
		Clinical trials	Venture capital

DNA/RNA or drug molecules, which is a common challenge, therefore requires a systematical study. To commercialize nanotechnologies for medical applications, new FDA policies, regulations and guidelines are being developed in the US, China and the rest of the world.

Despite the significant challenges and regulatory barriers in developing nanomedicine and its commercialization, huge progress has been made in nanomedicine over the last ten years and many nanotechnology-related clinical trials have been, or are being, conducted. Many commercial products based on nanomedicine approaches have emerged, and will continue to emerge, which may significantly impact on all areas of medicine. Nanomedicine will dramatically exceed what has occurred to date in the history of medicine, and will likely revolutionize medicine.

This work was supported by the National Heart Lung and Blood Institute of the National Institutes of Health (NIH) as a Program of Excellence in Nanotechnology Award (Grant No. HHSN268201000043C to Bao Gang) and by an NIH Nanomedicine Development Center Award (Grant No. PN2 EY018244 to Bao Gang).

1 Wgner V, Dullaart A, Bock A K, *et al*. The emerging nanomedicine landscape. Nat Biotechnol, 2006, 24: 1211–1217
2 Nie S M, Yun X, Gloria J K, *et al*. Nanotechnology Applications in Cancer. Ann Rev Biomed Eng, 2007, 9: 257–288
3 Kim B Y, Rutka J T, Chan W C. Nanomedicine. N Engl J Med, 2010, 363: 2434–2443
4 Smith A M, Gao X, Nie S. Quantum dot nanocrystals for *in vivo* molecular and cellular imaging. Photochem Photobiol, 2004, 80: 377–385
5 Nitin N, Santangelo P J, Kim G, *et al.* Peptide-linked molecular beacons for efficient delivery and rapid mRNA detection in living cells. Nucleic Acids Res, 2004, 32: e58
6 Nie S, Emory S R. Probing single molecules and single nanoparticles by surface-enhanced raman scattering. Science, 1997, 275: 1102–1106
7 Chan W C, Nie S. Quantum dot bioconjugates for ultrasensitive nonisotopic detection. Science, 1998, 281: 2016–2018
8 Emory S R, Haskins W E, Nie S. Direct observation of size-dependent optical enhancement in single metal nanoparticles. J Am Chem Soc, 1998, 120: 8009–8010
9 Han M, Gao X, Su J Z, *et al.* Quantum-dot-tagged microbeads for multiplexed optical coding of biomolecules. Nat Biotechnol, 2001, 19: 631–635
10 Chan W C, Maxwell D J, Gao X, *et al.* Luminescent quantum dots for multiplexed biological detection and imaging. Curr Opin Biotechnol, 2002, 13: 40–46
11 Gao X, Chan W C, Nie S. Quantum-dot nanocrystals for ultrasensitive biological labeling and multicolor optical encoding. J Biomed Opt, 2002, 7: 532–537
12 Bailey R E, Nie S. Alloyed semiconductor quantum dots: tuning the optical properties without changing the particle size. J Am Chem Soc, 2003, 125: 7100–7106
13 Gao X, Cui Y, Levenson R M, *et al. In vivo* cancer targeting and imaging with semiconductor quantum dots. Nat Biotechnol, 2004, 22: 969–976
14 Lidke D S, Nagy P, Heintzmann R, *et al.* Quantum dot ligands provide new insights into erbB/HER receptor-mediated signal transduction. Nat Biotechnol, 2004, 22: 198–203
15 Bruchez M, Moronne M, Gin P, *et al.* Semiconductor nanocrystals as fluorescent biological labels. Science, 1998, 281: 2013–2016
16 Akerman M E, Chan W C, Laakkonen P, *et al.* Nanocrystal targeting *in vivo*. Proc Natl Acad Sci USA, 2002, 99: 12617–12621
17 Dubertret B, Skourides P, Norris D J, *et al. In vivo* imaging of quantum dots encapsulated in phospholipid micelles. Science, 2002, 298: 1759–1762
18 Wu X, Liu H, Liu J, *et al.* Immunofluorescent labeling of cancer marker Her2 and other cellular targets with semiconductor quantum dots. Nat Biotechnol, 2003, 21: 41–46
19 Jaiswal J K, Mattoussi H, Mauro J M, *et al.* Long-term multiple color imaging of live cells using quantum dot bioconjugates. Nat Biotechnol, 2003, 21: 47–51
20 Larson D R, Zipfel W R, Williams R M, *et al.* Water-soluble quantum dots for multiphoton fluorescence imaging *in vivo*. Science, 2003, 300: 1434–1436
21 Ishii D, Kinbara K, Ishida Y, *et al.* Chaperonin-mediated stabilization and ATP-triggered release of semiconductor nanoparticles. Nature, 2003, 423: 628–632
22 Medintz I L, Clapp A R, Mattoussi H, *et al.* Self-assembled nanoscale biosensors based on quantum dot FRET donors. Nat Mater, 2003, 2: 630–638
23 Dahan M, Levi S, Luccardini C, *et al.* Diffusion dynamics of glycine receptors revealed by single-quantum dot tracking. Science, 2003, 302: 442–445
24 Voura E B, Jaiswal J K, Mattoussi H, *et al.* Tracking metastatic tumor cell extravasation with quantum dot nanocrystals and fluorescence emission-scanning microscopy. Nat Med, 2004, 10: 993–998
25 Garon E B, Marcu L, Luong Q, *et al.* Quantum dot labeling and tracking of human leukemic, bone marrow and cord blood cells. Leuk Res, 2007, 31: 643–651
26 Hama Y, Koyama Y, Urano Y, *et al.* Simultaneous two-color spectral fluorescence lymphangiography with near infrared quantum dots to map two lymphatic flows from the breast and the upper extremity. Breast Cancer Res Treat, 2007, 103: 23–28
27 Chattopadhyay P K, Price D A, Harper T F, *et al.* Quantum dot semiconductor nanocrystals for immunophenotyping by polychromatic flow cytometry. Nat Med, 2006, 12: 972–977
28 Howarth M, Takao K, Hayashi Y, *et al.* Targeting quantum dots to surface proteins in living cells with biotin ligase. Proc Natl Acad Sci USA, 2005, 102: 7583–7588
29 Bonasio R, Carman C V, Kim E, *et al.* Specific and covalent labeling of a membrane protein with organic fluorochromes and quantum dots. Proc Natl Acad Sci USA, 2007, 104: 14753–14758
30 Chang E, Miller J S, Sun J, *et al.* Protease-activated quantum dot probes. Biochem Biophys Res Commun, 2005, 334: 1317–1321
31 Xu C, Xing B, Rao J. A self-assembled quantum dot probe for detecting beta-lactamase activity. Biochem Biophys Res Commun, 2006, 344: 931–935
32 Clapp A R, Medintz I L, Uyeda H T, *et al.* Quantum dot-based multiplexed fluorescence resonance energy transfer. J Am Chem Soc, 2005, 127: 18212–18221
33 Yao H, Zhang Y, Xiao F, *et al.* Quantum dot/bioluminescence resonance energy transfer based highly sensitive detection of proteases. Angew Chem Int Ed, 2007, 46: 4346–4349
34 Medintz I L, Clapp A R, Brunel F M, *et al.* Proteolytic activity monitored by fluorescence resonance energy transfer through quantum-dot-peptide conjugates. Nat Mater, 2006, 5: 581–589
35 Goldman E R, Anderson G P, Tran P T, *et al.* Conjugation of luminescent quantum dots with antibodies using an engineered adaptor protein to provide new reagents for fluoroimmunoassays. Anal Chem, 2002, 74: 841–847
36 Wang Y A, Li J J, Chen H, *et al.* Stabilization of inorganic nanocrystals by organic dendrons. J Am Chem Soc, 2002, 124: 2293–2298
37 Chan W C W, Prendergast T L, Jain M, *et al.* One-step conjugation

of biomolecules to luminescent nanocrystals. Proc SPIE, 2000, 3924: 2–9
38 Pathak S, Choi S K, Arnheim N, *et al.* Hydroxylated quantum dots as luminescent probes for *in situ* hybridization. J Am Chem Soc, 2001, 123: 4103–4104
39 Mirkin C A, Letsinger R L, Mucic R C, *et al.* A DNA-based method for rationally assembling nanoparticles into macroscopic materials. Nature, 1996, 382: 607–609
40 Willard D M, Carillo L L, Jung J, *et al*. CdSe-ZnS quantum dots as resonance energy transfer donors in a model protein-protein binding assay. Nano Lett, 2001, 1: 469–474
41 Goldman E R, Balighian E D, Mattoussi H, *et al.* Avidin: a natural bridge for quantum dot-antibody conjugates. J Am Chem Soc, 2002, 124: 6378–6382
42 Rosenthal S J, Tomlinson I, Adkins E M, *et al.* Targeting cell surface receptors with ligand-conjugated nanocrystals. J Am Chem Soc, 2002, 124: 4586–4594
43 Dennis A M, Bao G. Quantum dot-fluorescent protein pairs as novel fluorescence resonance energy transfer probes. Nano Lett, 2008, 8: 1439–1445
44 Sapsford K E, Pons T, Medintz I L, *et al.* Biosensing with luminescent semiconductor quantum dots. Sensors-Basel, 2006, 6: 925–953
45 Qu L, Peng X. Control of photoluminescence properties of CdSe nanocrystals in growth. J Am Chem Soc, 2002, 124: 2049–2055
46 Striolo A, Ward J, Prausnitz J M, *et al.* Molecular weight, osmotic second virial coefficient, and extinction coefficient of colloidal CdSe nanocrystals. J Phys Chem B, 2002, 106: 5500–5505
47 Chan W C W, Maxwell D J, Gao X H, *et al.* Luminescent quantum dots for multiplexed biological detection and imaging. Curr Opin Biotech, 2002, 13: 40–46
48 Lakowicz J R. Principles of fluorescence spectroscopy. New York: Springer, 2006
49 Clapp A R, Medintz I L, Mattoussi H. Forster resonance energy transfer investigations using quantum-dot fluorophores. Chem Phys Chem, 2006, 7: 47–57
50 Sapsford K E, Pons T, Medintz I L, *et al.* Kinetics of metal-affinity driven self-assembly between proteins or peptides and CdSe-ZnS quantum dots. J Phys Chem C, 2007, 111: 11528–11538
51 Susumu K, Uyeda H T, Medintz I L, *et al.* Enhancing the stability and biological functionalities of quantum dots via compact multifunctional ligands. J Am Chem Soc, 2007, 129: 13987–13996
52 Shaner N C, Campbell R E, Steinbach P A, *et al.* Improved monomeric red, orange and yellow fluorescent proteins derived from Discosoma sp. red fluorescent protein. Nat Biotechnol, 2004, 22: 1567–1572
53 Shaner N C, Steinbach P A, Tsien R Y. A guide to choosing fluorescent proteins. Nat Methods, 2005, 2: 905–909
54 Busa W B, Nuccitelli R. Metabolic regulation via intracellular pH. Am J Physiol, 1984, 246: R409–R438
55 Tyagi S, Kramer F R. Molecular beacons: probes that fluoresce upon hybridization. Nat Biotechnol, 1996, 14: 303–308
56 Tyagi S, Bratu D P, Kramer F R. Multicolor molecular beacons for allele discrimination. Nat Biotechnol, 1998, 16: 49–53
57 Li J J, Geyer R, Tan W. Using molecular beacons as a sensitive fluorescence assay for enzymatic cleavage of single-stranded DNA. Nucleic Acids Res, 2000, 28: E52
58 Dirks R W, Molenaar C, Tanke H J. Methods for visualizing RNA processing and transport pathways in living cells. Histochem Cell Biol, 2001, 115: 3–11
59 Molenaar C, Marras S A, Slats J C, *et al*. Linear 2' O-Methyl RNA probes for the visualization of RNA in living cells. Nucleic Acids Res, 2001, 29: E89–89
60 Sokol D L, Zhang X, Lu P, *et al*. Real time detection of DNA.RNA hybridization in living cells. Proc Natl Acad Sci USA, 1998, 95: 11538–11543
61 Vet J A, Majithia A R, Marras S A, *et al*. Multiplex detection of four pathogenic retroviruses using molecular beacons. Proc Natl Acad Sci USA, 1999, 96: 6394–6399
62 Kostrikis L G, Tyagi S, Mhlanga M M, *et al*. Spectral genotyping of human alleles. Science, 1998, 279: 1228–1229
63 Piatek A S, Tyagi S, Pol A C, *et al*. Molecular beacon sequence analysis for detecting drug resistance in *Mycobacterium tuberculosis*. Nat Biotech, 1998, 16: 359–363
64 Bratu D P, Cha B J, Mhlanga M M, *et al*. Visualizing the distribution and transport of mRNAs in living cells. Proc Natl Acad Sci USA, 2003, 100: 13308–13313
65 Tsourkas A, Behlke M A, Xu Y, *et al*. Spectroscopic features of dual fluorescence/luminescence resonance energy-transfer molecular beacons. Anal Chem, 2003, 75: 3697–3703
66 Santangelo P J, Nix B, Tsourkas A, *et al*. Dual FRET molecular beacons for mRNA detection in living cells. Nucleic Acids Res, 2004, 32: e57
67 Nitin N, Santangelo P J, Kim G, *et al*. Peptide-linked molecular beacons for efficient delivery and rapid mRNA detection in living cells. Nucleic Acids Res, 2004, 32: e58
68 Tyagi S, Alsmadi O. Imaging native beta-actin mRNA in motile fibroblasts. Biophys J, 2004, 87: 4153–4162
69 Peng X H, Cao Z H, Xia J T, *et al*. Real-time detection of gene expression in cancer cells using molecular beacon imaging: new strategies for cancer research. Cancer Res, 2005, 65: 1909–1917
70 Medley C D, Drake T J, Tomasini J M, *et al*. Simultaneous monitoring of the expression of multiple genes inside of single breast carcinoma cells. Anal Chem, 2005, 77: 4713–4718
71 Tsourkas A, Behlke M A, Bao G. Structure-function relationships of shared-stem and conventional molecular beacons. Nucleic Acids Res, 2002, 30: 4208–4215
72 King F W, Liszewski W, Ritner C, *et al*. High-throughput tracking of pluripotent human embryonic stem cells with dual fluorescence resonance energy transfer molecular beacons. Stem Cells Dev, 2011, 20: 475–484
73 Chen A K, Rhee W J, Bao G, *et al*. Delivery of molecular beacons for live-cell imaging and analysis of RNA. Methods Mol Biol, 2011, 714: 159–174
74 Giles R V, Ruddell C J, Spiller D G, *et al*. Single base discrimination for ribonuclease H-dependent antisense effects within intact human leukaemia cells. Nucleic Acids Res, 1995, 23: 954–961
75 Barry M A, Eastman A. Identification of deoxyribonuclease II as an endonuclease involved in apoptosis. Arch Biochem Biophys, 1993, 300: 440–450
76 Giles R V, Spiller D G, Grzybowski J, *et al*. Selecting optimal oligonucleotide composition for maximal antisense effect following streptolysin O-mediated delivery into human leukaemia cells. Nucleic Acids Res, 1998, 26: 1567–1575
77 Walev I, Bhakdi S C, Hofmann F, *et al*. Delivery of proteins into living cells by reversible membrane permeabilization with streptolysin-O. Proc Natl Acad Sci USA, 2001, 98: 3185–3190
78 Wadia J S, Dowdy S F. Transmembrane delivery of protein and peptide drugs by TAT-mediated transduction in the treatment of cancer. Adv Drug Deliv Rev, 2005, 57: 579–596
79 Brooks H, Lebleu B, Vives E. Tat peptide-mediated cellular delivery: back to basics. Adv Drug Deliv Rev, 2005, 57: 559–577
80 Nitin N, Bao G. NLS peptide conjugated molecular beacons for visualizing nuclear RNA in living cells. Bioconj Chem, 2008, 19: 2205–2211
81 Czernin J, Allen-Auerbach M, Schelbert H. Improvements in cancer staging with PET/CT: literature-based evidence as of September 2006. J Nuclear Med, 2007, 48: 78S
82 Judenhofer M S, Wehrl H F, Newport D F, *et al.* Simultaneous PET-MRI: a new approach for functional and morphological imaging. Nat Med, 2008, 14: 459–465
83 Higuchi T, Anton M, Dumler K, *et al*. Combined reporter gene PET

and iron oxide MRI for monitoring survival and localization of transplanted cells in the rat heart. J Nucl Med, 2009, 50: 1088–1094
84 Xu H, Regino C A, Koyama Y, *et al*. Preparation and preliminary evaluation of a biotin-targeted, lectin-targeted dendrimer-based probe for dual-modality magnetic resonance and fluorescence imaging. Bioconjug Chem, 2007, 18: 1474–1482
85 Koyama Y, Talanov V S, Bernardo M, *et al*. A dendrimer-based nanosized contrast agent dual-labeled for magnetic resonance and optical fluorescence imaging to localize the sentinel lymph node in mice. J Magn Reson Imaging, 2007, 25: 866–871
86 Lee S K, Chen X. Dual-modality probes for *in vivo* molecular imaging. Mol Imaging, 2009, 8: 87–100
87 Carmeliet P. Angiogenesis in health and disease. Nat Med, 2003, 9: 653–660
88 Lee H Y, Li Z, Chen K, *et al.* PET/MRI dual-modality tumor imaging using arginine-glycine-aspartic (RGD)-conjugated radiolabeled iron oxide nanoparticles. J Nucl Med, 2008, 49: 1371–1379
89 Xie J, Huang J, Li X, *et al*. Iron oxide nanoparticle platform for biomedical applications. Curr Med Chem, 2009, 16: 1278–1294
90 Shokeen M, Fettig N M, Rossin R. Synthesis, *in vitro* and *in vivo* evaluation of radiolabeled nanoparticles. Q J Nucl Med Mol Imaging, 2008, 52: 267–277
91 Wang Y X, Hussain S M, Krestin G P. Superparamagnetic iron oxide contrast agents: physicochemical characteristics and applications in MR imaging. Eur Radiol, 2001, 11: 2319–2331
92 Bjornerud A, Wendland M F, Johansson L, *et al.* Use of intravascular contrast agents in MRI. Acad Radiol, 1998, 5: S223–225
93 Weissleder R, Bogdanov A, Neuwelt E A, *et al.* Long-circulating iron-oxides for MR imaging. Adv Drug Deliv Rev, 1995, 16: 321–334
94 Jun Y W, Huh Y M, Choi J S, *et al.* Nanoscale size effect of magnetic nanocrystals and their utilization for cancer diagnosis via magnetic resonance imaging. J Am Chem Soc, 2005, 127: 5732–5733
95 Xu C J, Sun S H. Monodisperse magnetic nanoparticles for biomedical applications. Polymer Int, 2007, 56: 821–826
96 Lee J H, Huh Y M, Jun Y W, *et al.* Artificially engineered magnetic nanoparticles for ultra-sensitive molecular imaging. Nat Med, 2007, 13: 95–99
97 Nitin N, LaConte L E, Zurkiya O, *et al.* Functionalization and peptide-based delivery of magnetic nanoparticles as an intracellular MRI contrast agent. J Biol Inorg Chem, 2004, 9: 706–712
98 Yu W W, Chang E, Sayes C M, *et al.* Aqueous dispersion of monodisperse magnetic iron oxide nanocrystals through phase transfer. Nanotechnology, 2006, 17: 4483–4487
99 Gossuin Y, Gillis P, Hocq A, *et al*. Magnetic resonance relaxation properties of superparamagnetic particles. Wiley Interdiscip Rev Nanomed Nanobiotechnol, 2009, 1: 299–310
100 Nahrendorf M, Jaffer F A, Kelly K A, *et al.* Noninvasive vascular cell adhesion molecule-1 imaging identifies inflammatory activation of cells in atherosclerosis. Circulation, 2006, 114: 1504–1511
101 Montet X, Montet-Abou K, Reynolds F, *et al.* Nanoparticle imaging of integrins on tumor cells. Neoplasia, 2006, 8: 214–222
102 Winter P M, Morawski A M, Caruthers S D, *et al.* Molecular imaging of angiogenesis in early-stage atherosclerosis with alpha(v)beta3-integrin-targeted nanoparticles. Circulation, 2003, 108: 2270–2274
103 Glaus C, Rossin R, Welch M J, *et al*. *In vivo* evaluation of ^{64}Cu-labeled magnetic nanoparticles as a dual-modality PET/MR imaging agent. Bioconjug Chem, 2010, 21: 715–722
104 Gillis P, Koenig S H. Transverse relaxation of solvent protons induced by magnetized spheres: application to ferritin, erythrocytes, and magnetite. Magn Reson Med, 1987, 5: 323–345
105 Gillis P, Moiny F, Brooks R A. On T_2-shortening by strongly magnetized spheres: a partial refocusing model. Magn Reson Med, 2002, 47: 257–263
106 Brooks R A, Moiny F, Gillis P. On T_2-shortening by weakly magnetized particles: the chemical exchange model. Magn Reson Med, 2001, 45: 1014–1020
107 Koenig S H, Kellar K E. Theory of $1/T_1$ and $1/T_2$ NMRD profiles of solutions of magnetic nanoparticles. Magn Reson Med, 1995, 34: 227–233
108 Jun Y W, Seo J W, Cheon A. Nanoscaling laws of magnetic nanoparticles and their applicabilities in biomedical sciences. Acc Chem Res, 2008, 41: 179–189
109 Tromsdorf U I, Bigall N C, Kaul M G, *et al.* Size and surface effects on the MRI relaxivity of manganese ferrite nanoparticle contrast agents. Nano Letters, 2007, 7: 2422–2427
110 Yu W W, Falkner J C, Yavuz C T, *et al.* Synthesis of monodisperse iron oxide nanocrystals by thermal decomposition of iron carboxylate salts. Chem Commun, 2004, 2306–2307
111 Xie J, Peng S, Brower N, *et al.* One-pot synthesis of monodisperse iron oxide nanoparticles for potential biomedical applications. Pure Appl Chem, 2006, 78: 1003–1014
112 Li J J, Wang Y A, Guo W Z, *et al.* Large-scale synthesis of nearly monodisperse CdSe/CdS core/shell nanocrystals using air-stable reagents via successive ion layer adsorption and reaction. J Am Chem Soc, 2003, 125: 12567–12575
113 Xie J, Xu C, Kohler N, *et al.* Controlled PEGylation of monodisperse Fe_3O_4 nanoparticles for reduced non-specific uptake by macrophage cells. Adv Mater, 2007, 19: 3163–3166
114 Torchilin V P, Trubetskoy V S. Which polymers can make nanoparticulate drug carriers long-circulating. Adv Drug Deliv Rev, 1995, 16: 141–155
115 Tong S, Hou S J, Zheng Z L, *et al.* Coating optimization of superparamagnetic iron oxide nanoparticles for high T_2 relaxivity. Nano Lett, 2010, 10: 4607–4613
116 Josephson L, Perez J M, Weissleder R. Magnetic nanosensors for the detection of oligonucleotide sequences. Angew Chem Int Edit, 2001, 40: 3204–3206
117 Hazarika P, Ceyhan B, Niemeyer C M. Reversible switching of DNA-gold nanoparticle aggregation. Angew Chem Int Edit, 2004, 43: 6469–6471
118 Montet X, Funovics M, Montet-Abou K, *et al.* Multivalent effects of RGD peptides obtained by nanoparticle display. J Med Chem, 2006, 49: 6087–6093
119 Pellegrino T, Manna L, Kudera S, *et al.* Hydrophobic nanocrystals coated with an amphiphilic polymer shell: A general route to water soluble nanocrystals. Nano Lett, 2004, 4: 703–707
120 Stolnik S, Illum L, Davis S S. Long circulating microparticulate drug carriers. Adv Drug Deliv Rev, 1995, 16: 195–214
121 Liu Z, Davis C, Cai W, *et al.* Circulation and long-term fate of functionalized, biocompatible single-walled carbon nanotubes in mice probed by Raman spectroscopy. Proc Natl Acad Sci USA, 2008, 105: 1410–1415
122 Glaus C, Rossin R, Welch M J, *et al*. *In vivo* evaluation of ^{64}Cu-labeled magnetic nanoparticles as a dual-modality PET/MR imaging agent. Bioconjug Chem, 2010, 21: 715–722
123 Torchilin V P. PEG-based micelles as carriers of contrast agents for different imaging modalities. Adv Drug Deliv Rev, 2002, 54: 235–252
124 Johnsson M, Hansson P, Edwards K. Spherical micelles and other self-assembled structures in dilute aqueous mixtures of poly(ethylene glycol) lipids. J Phys Chem B, 2001, 105: 8420–8430
125 Turro N J, Yekta A. Luminescent probes for detergent solutions—simple procedure for determination of mean aggregation number of micelles. J Am Chem Soc, 1978, 100: 5951–5952
126 Tong S, Hou S, Ren B, *et al*. Self-assembly of phospholipid-PEG coating on nanoparticles through dual solvent exchange. Nano Lett, 2011, 11: 3720–3726
127 Zhu M T, Wang B, Wang Y, *et al*. Endothelial dysfunction and inflammation induced by iron oxide nanoparticle exposure: Risk factors for early atherosclerosis. Toxicol Lett, 2011, 203: 162–171
128 Hyafil F, Cornily J C, Feig J E, *et al.* Noninvasive detection of

macrophages using a nanoparticulate contrast agent for computed tomography. Nat Med, 2007, 13: 636–641
129 Haller C, Hizoh I. The cytotoxicity of iodinated radiocontrast agents on renal cells *in vitro*. Invest Radiol, 2004, 39: 149–154
130 Kong W H, Lee W J, Cui Z Y, *et al.* Nanoparticulate carrier containing water-insoluble iodinated oil as a multifunctional contrast agent for computed tomography imaging. Biomaterials, 2007, 28: 5555–5561
131 Badea C T, Athreya K K, Espinosa G, *et al.* Computed tomography imaging of primary lung cancer in mice using a liposomal-iodinated contrast agent. PLoS ONE, 2012, 7: e34496
132 Hoglund P, Leander P, Hustvedt S O, *et al.* Human pharmacokinetics and modeling of the concentration-attenuation relationship of a new liposomal liver-specific contrast agent for CT. Acad Radiol, 1998, 5: S47–S48
133 Kim D, Park S, Lee J H, *et al.* Antibiofouling polymer-coated gold nanoparticles as a contrast agent for in vivo x-ray computed tomography imaging. J Am Chem Soc, 2007, 129: 7661–7665
134 Wang H, Zheng L F, Guo R, *et al.* Dendrimer-entrapped gold nanoparticles as potential CT contrast agents for blood pool imaging. Nanoscale Res Lett, 2012, 7: 190–197
135 Liu H, Wang H, Guo R, *et al.* Size-controlled synthesis of dendrimer-stabilized silver nanoparticles for X-ray computed tomography imaging applications. Polym Chem-UK, 2010, 1: 1677–1683
136 Rabin O, Perez J M, Grimm J, *et al.* An X-ray computed tomography imaging agent based on long-circulating bismuth sulphide nanoparticles. Nat Mater, 2006, 5: 118–122
137 Ai K L, Liu Y L, Liu J H, *et al.* Large-scale synthesis of Bi2S3 nanodots as a contrast agent for *in vivo* X-ray computed tomography imaging. Adv Mater, 2011, 23: 4886–4891
138 Kinsella J M, Jimenez R E, Karmali P P, *et al.* X-Ray computed tomography imaging of breast cancer by using targeted peptide-labeled bismuth sulfide nanoparticles. Angew Chem Int Edit, 2011, 50: 12308–12311
139 Oh M H, Lee N, Kim H, *et al.* Large-scale synthesis of bioinert tantalum oxide nanoparticles for X-ray computed tomography imaging and bimodal image-guided sentinel lymph node mapping. J Am Chem Soc, 2011, 133: 5508–5515
140 Lee N, Cho H R, Oh M H, *et al.* Multifunctional Fe_3O_4/TaO_x core/shell nanoparticles for simultaneous magnetic resonance imaging and X-ray computed tomography. J Am Chem Soc, 2012, 134: 10309–10312
141 Jain R K. Delivery of molecular and cellular medicine to solid tumors. Adv Drug Deliv Rev, 2001, 46: 149–168
142 von Maltzahn G, Park J H, Lin K Y, *et al.* Nanoparticles that communicate *in vivo* to amplify tumour targeting. Nat Mater, 2011, 10: 545–552
143 Weissleder R, Stark D D, Engelstad B L, *et al.* Superparamagnetic iron oxide: pharmacokinetics and toxicity. AJR Am J Roentgenol, 1989, 152: 167–173
144 Namiki Y, Namiki T, Yoshida H, *et al.* A novel magnetic crystal-lipid nanostructure for magnetically guided *in vivo* gene delivery. Nat Nanotechnol, 2009, 4: 598–606
145 Fortin J P, Wilhelm C, Servais J, *et al.* Size-sorted anionic iron oxide nanomagnets as colloidal mediators for magnetic hyperthermia. J Am Chem Soc, 2007, 129: 2628–2635
146 Alexiou C, Arnold W, Klein R J, *et al.* Locoregional cancer treatment with magnetic drug targeting. Cancer Res, 2000, 60: 6641–6648
147 Park J H, von Maltzahn G, Ruoslahti E, *et al.* Micellar hybrid nanoparticles for simultaneous magnetofluorescent imaging and drug delivery. Angew Chem Int Edit, 2008, 47: 7284–7288
148 Jain T K, Richey J, Strand M, *et al.* Magnetic nanoparticles with dual functional properties: drug delivery and magnetic resonance imaging. Biomaterials, 2008, 29: 4012–4021
149 Guthi J S, Yang S G, Huang G, *et al.* MRI-visible micellar nanomedicine for targeted drug delivery to lung cancer cells. Mol Pharm, 2010, 7: 32–40
150 Liong M, Lu J, Kovochich M, *et al.* Multifunctional inorganic nanoparticles for imaging, targeting, and drug delivery. ACS Nano, 2008, 2: 889–896
151 Dilnawaz F, Singh A, Mohanty C, *et al.* Dual drug loaded superparamagnetic iron oxide nanoparticles for targeted cancer therapy. Biomaterials, 2010, 31: 3694–3706
152 Santra S, Kaittanis C, Grimm J, *et al.* Drug/dye-loaded, multifunctional iron oxide nanoparticles for combined targeted cancer therapy and dual optical/magnetic resonance imaging. Small, 2009, 5: 1862–1868
153 Kim J, Kim H S, Lee N, *et al.* Multifunctional uniform nanoparticles composed of a magnetite nanocrystal core and a mesoporous silica shell for magnetic resonance and fluorescence imaging and for drug delivery. Angew Chem Int Ed Engl, 2008, 47: 8438–8441
154 Nobuto H, Sugita T, Kubo T, *et al.* Evaluation of systemic chemotherapy with magnetic liposomal doxorubicin and a dipole external electromagnet. Int J Cancer, 2004, 109: 627–635
155 Medarova Z, Pham W, Farrar C, *et al. In vivo* imaging of siRNA delivery and silencing in tumors. Nat Med, 2007, 13: 372–377
156 Lee J H, Lee K, Moon S H, *et al.* All-in-one target-cell-specific magnetic nanoparticles for simultaneous molecular imaging and siRNA delivery. Angew Chem Int Ed Engl, 2009, 48: 4174–4179
157 Shin J M, Anisur R M, Ko M K, *et al.* Hollow manganese oxide nanoparticles as multifunctional agents for magnetic resonance imaging and drug delivery. Angew Chem Int Edit, 2009, 48: 321–324
158 Choi J S, Lee J H, Shin T H, *et al.* Self-confirming "AND" logic nanoparticles for fault-free MRI. J Am Chem Soc, 2010, 132: 11015–11017
159 Bartlett D W, Su H, Hildebrandt I J, *et al.* Impact of tumor-specific targeting on the biodistribution and efficacy of siRNA nanoparticles measured by multimodality in vivo imaging. Proc Natl Acad Sci USA, 2007, 104: 15549–15554
160 Chen W, Xu N, Xu L, *et al.* Multifunctional magnetoplasmonic nanoparticle assemblies for cancer therapy and diagnostics (theranostics). Macromol Rapid Commun, 2010, 31: 228–236
161 Hu J, Qian Y, Wang X, *et al.* Drug-loaded and superparamagnetic iron oxide nanoparticle surface-embedded amphiphilic block copolymer micelles for integrated chemotherapeutic drug delivery and MR imaging. Langmuir, 2012, 28: 2073–2082
162 Kopelman R, Koo Y E L, Philbert M, *et al.* Multifunctional nanoparticle platforms for *in vivo* MRI enhancement and photodynamic therapy of a rat brain cancer. J Magn Magn Mater, 2005, 293: 404–410
163 Zheng J, Allen C, Serra S, *et al.* Liposome contrast agent for CT-based detection and localization of neoplastic and inflammatory lesions in rabbits: validation with FDG-PET and histology. Contrast Media Mol Imag, 2010, 5: 147–154
164 Barth B M, Sharma R, Altinoglu E I, *et al.* Bioconjugation of calcium phosphosilicate composite nanoparticles for selective targeting of human breast and pancreatic cancers *in vivo*. ACS Nano, 2010, 4: 1279–1287
165 Guo R, Zhang L, Qian H, *et al.* Multifunctional nanocarriers for cell imaging, drug delivery, and near-IR photothermal therapy. Langmuir, 2010, 26: 5428–5434
166 Lin X, Xie J, Niu G, *et al.* Chimeric ferritin nanocages for multiple function loading and multimodal imaging. Nano Lett, 2011, 11: 814–819
167 Jain T K, Morales M A, Sahoo S K, *et al.* Iron oxide nanoparticles for sustained delivery of anticancer agents. Mol Pharm, 2005, 2: 194–205
168 Dames P, Gleich B, Flemmer A, *et al.* Targeted delivery of magnetic aerosol droplets to the lung. Nat Nanotechnol, 2007, 2: 495–499
169 Wood A J, Lo T W, Zeitler B, *et al*. Targeted genome editing across species using ZFNs and TALENs. Science, 2011, 333: 307

170 Boch J, Scholze H, Schornack S, *et al.* Breaking the code of DNA binding specificity of TAL-type III effectors. Science, 2009, 326: 1509–1512
171 Porteus M H, Baltimore D. Chimeric nucleases stimulate gene targeting in human cells. Science, 2003, 300: 763
172 Rouet P, Smih F, Jasin M. Expression of a site-specific endonuclease stimulates homologous recombination in mammalian cells. Proc Natl Acad Sci USA, 1994, 91: 6064–6068
173 Bitinaite J, Wah D A, Aggarwal A K, *et al.* Fok I dimerization is required for DNA cleavage. Proc Natl Acad Sci USA, 1998, 95: 10570–10575
174 Smith J, Bibikova M, Whitby F G, *et al.* Requirements for double-strand cleavage by chimeric restriction enzymes with zinc finger DNA-recognition domains. Nucleic Acids Res, 2000, 28: 3361–3369
175 Moscou M J, Bogdanove A J. A simple cipher governs DNA recognition by TAL effectors. Science, 2009, 326: 1501
176 Cradick T J, Ambrosini G, Iseli C, *et al.* ZFN-site searches genomes for zinc finger nuclease target sites and off-target sites. BMC Bioinformatics, 2011, 12: 152
177 Miller J C, Holmes M C, Wang J, *et al.* An improved zinc-finger nuclease architecture for highly specific genome editing. Nat Biotechnol, 2007, 25: 778–785
178 Ramirez C L, Certo M T, Mussolino C, *et al.* Engineered zinc finger nickases induce homology-directed repair with reduced mutagenic effects. Nucleic Acids Res, 2012, 40: 5560–5568
179 Perez E E, Wang J, Miller J C, *et al*. Establishment of HIV-1 resistance in $CD4^+$ T cells by genome editing using zinc-finger nucleases. Nat Biotechnol, 2008, 26: 808–816
180 Platt O S, Brambilla D J, Rosse W F, *et al*. Mortality in sickle cell disease. Life expectancy and risk factors for early death. N Engl J Med, 1994, 330: 1639–1644